

UNIVERSIDAD DE CONCEPCIÓN



CENTRO DE INVESTIGACIÓN EN
INGENIERÍA MATEMÁTICA (CI²MA)



Numerical approximation of a potentials formulation for the
elasticity vibration problem

JORGE ALBELLA, RODOLFO RODRÍGUEZ,
PABLO VENEGAS

PREPRINT 2022-28

SERIE DE PRE-PUBLICACIONES

Numerical approximation of a potentials formulation for the elasticity vibration problem.

J. Albella^a, R. Rodríguez^b, P. Venegas^c

^a*Departamento de Didácticas Aplicadas, Universidade de Santiago de Compostela, E-15782 Santiago de Compostela, Spain*

^b*CP²MA, Departamento de Ingeniería Matemática, Universidad de Concepción, Concepción, Chile*

^c*GIMNAP, Departamento de Matemática, Universidad del Bío-Bío, Concepción, Chile*

Abstract

This paper deals with a numerical approximation of the elasticity vibration problem based on a potentials decomposition. Decomposing the displacements field into potentials is a well-known tool in elastodynamics that takes advantage of the decoupling of pressure waves and shear waves inside a homogeneous isotropic media. In the spectral problem on a bounded domain, this decomposition decouples the elasticity equations into two Laplacian-like equations that only interact at the boundary. We show that spurious eigenvalues appear when Lagrangian finite elements are used to discretize the problem. Then, we propose an alternative weak formulation which avoids this drawback. A finite element discretization of this weak formulation based again on Lagrangian finite elements is proposed and tested by means of some numerical experiments, which show convergence and absence of spurious modes.

Keywords: Spectral elasticity problem, Helmholtz decomposition, Potentials, Finite element method

1. Introduction

The aim of this paper is to study the numerical approximation of a potentials formulation for the elasticity vibration problem. More precisely, we focus on the following

Email addresses: jorge.albella@usc.es (J. Albella), rodolfo@ing-mat.udec.cl (R. Rodríguez), pvenegas@ubiobio.cl (P. Venegas)

two-dimensional eigenvalue problem: find (ω, \mathbf{u}) , such that

$$-\frac{\lambda + 2\mu}{\rho} \nabla(\operatorname{div} \mathbf{u}) + \frac{\mu}{\rho} \mathbf{curl}(\operatorname{curl} \mathbf{u}) = \omega^2 \mathbf{u} \quad \text{in } \Omega, \quad (1.1a)$$

$$\mathbf{u} = 0 \quad \text{on } \partial\Omega, \quad (1.1b)$$

where $\Omega \subset \mathbb{R}^2$ is the reference domain (which is assumed to be a Lipschitz-continuous, bounded, and convex open subset), \mathbf{u} is the displacement field, ω is the vibration frequency, ρ is the (assumed constant) material density, and $\lambda > 0$ and $\mu > 0$ are the Lamé coefficients (also assumed constant). We also use the two-dimensional curl operators defined by $\operatorname{curl} \mathbf{u} = \partial_x u_2 - \partial_y u_1$ for the scalar curl of a vector field $\mathbf{u} = (u_1, u_2)$ and $\mathbf{curl} \varphi = (\partial_y \varphi, -\partial_x \varphi)$ for the vector curl of a scalar field φ . Let us remark that here and thereafter, we use bold symbols to denote vector fields, vector valued functions and vector spaces.

It is well known that there exist many numerical methods to solve these equations. However, the use of the Helmholtz decomposition of vector fields in terms of potentials for numerical purposes, which appears in other areas such as electromagnetism or fluid mechanics, has not been used in this context. Let us remark that decomposing a given field into potentials makes it possible to solve a problem with fewer unknowns and to reduce it to partial differential equations with a simpler form, such as Poisson or D'Alembert equations, for example.

In the elastodynamics setting, such a decomposition relates elastodynamic equations to two wave equations and enlightens the decomposition of the wave field as the sum of pressure waves (P waves, that are gradients of a pressure potential) and shear waves (S waves, that are curls of a shear potential), which propagate independently with different velocities in the interior of the domain, the velocity of the P waves being larger than that of the S waves. The main difficulty of this approach is to cope with the coupling of these two kind of waves (the so-called conversion of modes), which occurs due to wave reflections and transmissions at interfaces between homogeneous media or at physical boundaries.

Until recently, very few works have been devoted to the exploitation of this idea for finite element computations in elastodynamics; see [8, 2, 3]. In particular, a finite element discretization has been considered in [8] in the case of Dirichlet boundary conditions. Following the same idea, the challenging case of free surface boundary conditions has been studied in [2, 3], where it has been shown that some severe stability issues must be dealt with if a straightforward approach is used. To the best of the author's knowledge, this approach has not been considered in the spectral setting.

Following the approach introduced in the previous references, a potentials formulation of problem (1.1) could be in principle discretized by Lagrangian finite elements of the same

kind for both potentials. However, we report numerical evidence showing that this naive discretization introduces spurious eigenvalues interspersed among the approximations of the actual eigenvalues of the elasticity problem. The reason for this is that this potentials formulation has $\omega^2 = 0$ as a spurious eigenvalue with an infinite-dimensional eigenspace (the so called *kernel*), which is not well represented in the corresponding discretization.

To avoid this drawback, we propose in this paper a new variational formulation of (1.1) whose discretization will be free of spurious eigenvalues. With this aim, we first characterize the kernel of this formulation, which is used to define an equivalent mixed formulation. For its numerical approximation, we propose a discretization based on Lagrangian finite elements for the potentials combined with a suitable discretization of the kernel.

The outline of the paper is as follows. In Section 2, we introduce the potentials decomposition and some function spaces that will be used in what follows. We also show that spurious eigenvalues appear when standard Lagrangian finite elements are used to discretize a potentials formulation of the elasticity vibration problem (1.1). Then, in Section 3, we propose an alternative weak formulation and prove that it is equivalent to the spectral problem for a self-adjoint compact operator. This allows us to obtain a thorough characterization of the solutions of the proposed formulation. In Section 4, we introduce a finite element discretization of this formulation and in Section 5 we report some numerical tests that allow us to assess the convergence of the method and to check that it is not polluted with spurious modes. We end the paper with an appendix, where we describe an alternative implementation of the discrete problem based on a mixed formulation that avoids the discretization of the kernel. The appendix also includes the proof of the equivalence between this new mixed problem and the continuous problem previously analyzed.

2. Model problem and potentials formulation

To make this paper self contained, first we recap in this section how to reduce the solution of the elasticity vibration problem (1.1) to two scalar spectral problems coupled at the boundary. With this aim, we proceed as in [2] and introduce two scalar potentials, φ_P and φ_S , which will be used to write a Helmholtz decomposition of the displacement field \mathbf{u} :

$$\varphi_P := V_P^2 \operatorname{div} \mathbf{u} \quad \text{and} \quad \varphi_S := -V_S^2 \operatorname{curl} \mathbf{u} \quad \text{in } \Omega, \quad (2.1)$$

where

$$V_P^2 := \frac{\lambda + 2\mu}{\rho} \quad \text{and} \quad V_S^2 := \frac{\mu}{\rho}$$

are, respectively, the squared velocities of the P and the S waves in the elastodynamics setting.

From the above equations and (1.1a), it follows that

$$-\omega^2 \mathbf{u} = \nabla \varphi_P + \mathbf{curl} \varphi_S, \quad (2.2)$$

which provides a Helmholtz decomposition of the vector field $-\omega^2 \mathbf{u}$. To obtain the equations satisfied by these potentials, we simply substitute (2.2) into (2.1):

$$-V_P^2 \Delta \varphi_P = \omega^2 \varphi_P \quad \text{and} \quad -V_S^2 \Delta \varphi_S = \omega^2 \varphi_S \quad \text{in } \Omega, \quad (2.3)$$

where we have used the identity $\mathbf{curl}(\mathbf{curl} \varphi_S) = -\Delta \varphi_S$. The above equations, which are totally decoupled in Ω , must be completed with appropriate boundary conditions to take into account (1.1b), namely,

$$\nabla \varphi_P + \mathbf{curl} \varphi_S = \mathbf{0} \quad \text{on } \partial\Omega. \quad (2.4)$$

Conversely, it is easy to check that if $(\omega, \varphi_P, \varphi_S)$ with $\omega > 0$ is a solution of (2.3)–(2.4), then (ω, \mathbf{u}) with $\mathbf{u} := \nabla \varphi_P + \mathbf{curl} \varphi_S$ satisfies (1.1).

To propose a variational formulation of (2.3)–(2.4), first we rewrite the boundary condition as follows:

$$\nabla \varphi_P + \mathbf{curl} \varphi_S = \mathbf{0} \quad \text{on } \partial\Omega \iff \begin{cases} (\nabla \varphi_P + \mathbf{curl} \varphi_S) \cdot \mathbf{n} = 0 & \text{on } \partial\Omega, \\ (\nabla \varphi_P + \mathbf{curl} \varphi_S) \cdot \mathbf{t} = 0 & \text{on } \partial\Omega, \end{cases}$$

where $\mathbf{n} := (n_1, n_2)$ and $\mathbf{t} = (n_2, -n_1)$ denote unit normal and tangential vectors to $\partial\Omega$, respectively. This leads to the following coupled boundary conditions for φ_S and φ_P :

$$\partial_{\mathbf{n}} \varphi_P = \partial_{\mathbf{t}} \varphi_S \quad \text{and} \quad \partial_{\mathbf{n}} \varphi_S = -\partial_{\mathbf{t}} \varphi_P \quad \text{on } \partial\Omega. \quad (2.5)$$

Multiplying the two equations in (2.3) by smooth test functions ψ_P and ψ_S , respectively, integrating by parts and using the equations above for the boundary terms, we can write

$$a((\varphi_P, \varphi_S), (\psi_P, \psi_S)) = \omega^2 m((\varphi_P, \varphi_S), (\psi_P, \psi_S)), \quad (2.6)$$

where

$$a((\varphi_P, \varphi_S), (\psi_P, \psi_S)) := \int_{\Omega} \nabla \varphi_P \cdot \nabla \psi_P + \int_{\Omega} \nabla \varphi_S \cdot \nabla \psi_S + \int_{\partial\Omega} (\partial_{\mathbf{t}} \varphi_P \psi_S + \partial_{\mathbf{t}} \psi_P \varphi_S) \quad (2.7)$$

and

$$m((\varphi_P, \varphi_S), (\psi_P, \psi_S)) := \int_{\Omega} \frac{1}{V_P^2} \varphi_P \psi_P + \int_{\Omega} \frac{1}{V_S^2} \varphi_S \psi_S. \quad (2.8)$$

Notice that the essential boundary condition (1.1b) for the displacement formulation becomes two natural conditions for this potentials formulation.

It remains to find an adequate space to pose problem (2.6). With this end, we resort to the following lemma, whose proof can be found in [2].

Lemma 2.1. *For all $(\varphi_P, \varphi_S), (\psi_P, \psi_S) \in \mathbf{H}^1(\Omega)$,*

$$a((\varphi_P, \varphi_S), (\psi_P, \psi_S)) = \int_{\Omega} (\nabla \varphi_P + \mathbf{curl} \varphi_S) \cdot (\nabla \psi_P + \mathbf{curl} \psi_S).$$

This lemma suggests that the appropriate space to pose problem (2.6) is not $\mathbf{H}^1(\Omega)$ but

$$\mathbf{V} := \{ \boldsymbol{\psi} = (\psi_P, \psi_S)^\top \in \mathbf{L}^2(\Omega) : \nabla \psi_P + \mathbf{curl} \psi_S \in \mathbf{L}^2(\Omega) \}.$$

In this space, the bilinear form $a(\cdot, \cdot)$ can be written as in this lemma, which allows us to avoid dealing with the boundary terms in (2.7) for the analysis. In fact, we will show below that problem (2.6) posed on \mathbf{V} turns out to be equivalent to a variational formulation of (1.1).

On the other hand, for all $\boldsymbol{\psi} = (\psi_P, \psi_S) \in \mathbf{V}$, it is easy to check that

$$\nabla \psi_P + \mathbf{curl} \psi_S = \begin{pmatrix} \operatorname{div} \boldsymbol{\psi} \\ -\operatorname{curl} \boldsymbol{\psi} \end{pmatrix}. \quad (2.9)$$

Thus, \mathbf{V} can also be written as

$$\mathbf{V} = \mathbf{H}(\operatorname{div}, \Omega) \cap \mathbf{H}(\operatorname{curl}, \Omega),$$

which is a Hilbert space endowed with its natural norm:

$$\|\boldsymbol{\psi}\|_{\mathbf{V}}^2 := \|\operatorname{div} \boldsymbol{\psi}\|_{\mathbf{L}^2(\Omega)}^2 + \|\operatorname{curl} \boldsymbol{\psi}\|_{\mathbf{L}^2(\Omega)}^2 + \|\boldsymbol{\psi}\|_{\mathbf{L}^2(\Omega)}^2.$$

We also introduce the corresponding semi-norm, which will be used in the sequel:

$$|\boldsymbol{\psi}|_{\mathbf{V}}^2 := \|\operatorname{div} \boldsymbol{\psi}\|_{\mathbf{L}^2(\Omega)}^2 + \|\operatorname{curl} \boldsymbol{\psi}\|_{\mathbf{L}^2(\Omega)}^2.$$

Notice that \mathbf{V} clearly contains $\mathbf{H}^1(\Omega)$. Moreover the following density result holds true (see [4, Proposition 2.3]).

Proposition 2.2. *The space \mathbf{V} strictly contains $\mathbf{H}^1(\Omega)$. Moreover, the space $\mathcal{D}(\overline{\Omega})^2$ and thus the space $\mathbf{H}^1(\Omega)$ are dense in \mathbf{V} .*

Now, we are in a position to pose the variational eigenvalue problem:

Problem 1. Find $(\omega, \boldsymbol{\varphi}) \in \mathbb{R}^+ \times \mathbf{V}$ such that $\boldsymbol{\varphi} \neq \mathbf{0}$ and

$$a(\boldsymbol{\varphi}, \boldsymbol{\psi}) = \omega^2 m(\boldsymbol{\varphi}, \boldsymbol{\psi}) \quad \forall \boldsymbol{\psi} \in \mathbf{V}. \quad (2.10)$$

In this eigenvalue problem, thanks to (2.9), the bilinear form $a(\cdot, \cdot)$ can be written as

$$a(\boldsymbol{\varphi}, \boldsymbol{\psi}) = \int_{\Omega} \operatorname{div} \boldsymbol{\varphi} \operatorname{div} \boldsymbol{\psi} + \int_{\Omega} \operatorname{curl} \boldsymbol{\varphi} \operatorname{curl} \boldsymbol{\psi}, \quad \boldsymbol{\varphi}, \boldsymbol{\psi} \in \mathbf{V},$$

while $m(\cdot, \cdot)$ remains as originally defined in (2.8):

$$m(\boldsymbol{\varphi}, \boldsymbol{\psi}) = \int_{\Omega} \frac{1}{V_P^2} \varphi_P \psi_P + \int_{\Omega} \frac{1}{V_S^2} \varphi_S \psi_S, \quad \boldsymbol{\varphi}, \boldsymbol{\psi} \in \mathbf{L}^2(\Omega).$$

Remark 2.3. The variational formulation above can also be obtained from (2.9) and (2.4) by imposing the boundary conditions

$$\operatorname{div} \boldsymbol{\varphi} = 0 \quad \text{and} \quad \operatorname{curl} \boldsymbol{\varphi} = 0 \quad \text{on } \partial\Omega.$$

instead of (2.5); see [1] for details.

Next, we prove that, when $\omega > 0$, Problem 1 is actually equivalent to the standard variational formulation of problem (1.1), which reads as follows:

Problem 2. Find $(\omega, \mathbf{u}) \in \mathbb{R}^+ \times \mathbf{H}_0^1(\Omega)$ such that $\mathbf{u} \neq \mathbf{0}$ and

$$\int_{\Omega} V_P^2 \operatorname{div} \mathbf{u} \operatorname{div} \mathbf{v} + \int_{\Omega} V_S^2 \operatorname{curl} \mathbf{u} \operatorname{curl} \mathbf{v} = \omega^2 \int_{\Omega} \mathbf{u} \cdot \mathbf{v} \quad \forall \mathbf{v} \in \mathbf{H}_0^1(\Omega). \quad (2.11)$$

For any solution of this problem, it is easy to check that $\omega > 0$. In what follows, we prove that, in such a case, Problems 1 and 2 are equivalent.

Lemma 2.4. If $(\omega, \boldsymbol{\varphi})$ with $\omega > 0$ and $\boldsymbol{\varphi} = (\varphi_P, \varphi_S)^\top$ is a solution to Problem 1, then (ω, \mathbf{u}) with $\mathbf{u} := \nabla \varphi_P + \operatorname{curl} \varphi_S$ is a solution to Problem 2. Conversely, if (ω, \mathbf{u}) is a solution to Problem 2, then $(\omega, \boldsymbol{\varphi})$ with $\boldsymbol{\varphi} := (V_P^2 \operatorname{div} \mathbf{u}, -V_S^2 \operatorname{curl} \mathbf{u})^\top$ is a solution to Problem 1.

PROOF. Let $(\omega, \boldsymbol{\varphi})$ be a solution to Problem 1 with $\omega > 0$ and $\boldsymbol{\varphi} = (\varphi_P, \varphi_S)^\top$. Let $\mathbf{u} := \nabla\varphi_P + \mathbf{curl}\varphi_S$. Then, from (2.9) and (2.10) we have

$$\int_{\Omega} \mathbf{u} \cdot (\nabla\psi_P + \mathbf{curl}\psi_S) = \omega^2 \left(\int_{\Omega} \frac{1}{V_P^2} \varphi_P \psi_P + \int_{\Omega} \frac{1}{V_S^2} \varphi_S \psi_S \right) \quad \forall \boldsymbol{\psi} = (\psi_P, \psi_S)^\top \in \mathbf{V}.$$

Since $\mathcal{D}(\Omega)^2$ and $\mathcal{D}(\overline{\Omega})^2$ are subsets of \mathbf{V} , straightforward computations yield

$$-\operatorname{div} \mathbf{u} = \omega^2 \frac{\varphi_P}{V_P^2} \quad \text{in } \Omega \quad \text{and} \quad \mathbf{u} \cdot \mathbf{n} = 0 \quad \text{on } \partial\Omega,$$

as well as

$$\operatorname{curl} \mathbf{u} = \omega^2 \frac{\varphi_S}{V_S^2} \quad \text{in } \Omega \quad \text{and} \quad \mathbf{u} \cdot \mathbf{t} = 0 \quad \text{on } \partial\Omega.$$

Therefore, $\mathbf{u} \in \mathbf{H}_0(\operatorname{div}, \Omega) \cap \mathbf{H}_0(\operatorname{curl}, \Omega) = \mathbf{H}_0^1(\Omega)$ (see [9, Lemma 2.5]). Moreover,

$$\begin{aligned} -V_P^2 \nabla(\operatorname{div} \mathbf{u}) + V_S^2 \mathbf{curl}(\operatorname{curl} \mathbf{u}) &= \omega^2 (\nabla\varphi_P + \mathbf{curl}\varphi_S) = \omega^2 \mathbf{u} \quad \text{in } \Omega, \\ \mathbf{u} &= \mathbf{0} \quad \text{on } \partial\Omega. \end{aligned}$$

Then, (ω, \mathbf{u}) is a solution to (1.1) and, hence, to Problem 2, which is just its variational formulation.

Conversely, let (ω, \mathbf{u}) be a solution to Problem 2. We set $\varphi_P := V_P^2 \operatorname{div} \mathbf{u}$ and $\varphi_S := -V_S^2 \operatorname{curl} \mathbf{u}$. Then, from (2.11), it follows that

$$\int_{\Omega} \varphi_P \operatorname{div} \mathbf{v} - \int_{\Omega} \varphi_S \operatorname{curl} \mathbf{v} = \omega^2 \int_{\Omega} \mathbf{u} \cdot \mathbf{v} \quad \forall \mathbf{v} \in \mathbf{H}_0^1(\Omega).$$

Hence, taking $\mathbf{v} \in \mathcal{D}(\Omega)^2$ and integrating by parts yield

$$-\omega^2 \mathbf{u} = \nabla\varphi_P + \mathbf{curl}\varphi_S = \begin{pmatrix} \operatorname{div} \boldsymbol{\varphi} \\ -\operatorname{curl} \boldsymbol{\varphi} \end{pmatrix} \quad \text{in } \Omega, \quad (2.12)$$

the last equality because of (2.9).

On the other hand, let us write $\mathbf{u} = (u_1, u_2)^\top$. From (2.9) again and the definition of $\boldsymbol{\varphi}$,

$$\nabla u_1 + \mathbf{curl} u_2 = \begin{pmatrix} \operatorname{div} \mathbf{u} \\ -\operatorname{curl} \mathbf{u} \end{pmatrix} = \begin{pmatrix} \varphi_P/V_P^2 \\ \varphi_S/V_S^2 \end{pmatrix}.$$

Consequently,

$$\int_{\Omega} (\nabla u_1 + \mathbf{curl} u_2) \cdot \boldsymbol{\psi} = \int_{\Omega} \frac{1}{V_P^2} \varphi_P \psi_P + \int_{\Omega} \frac{1}{V_S^2} \varphi_S \psi_S \quad \forall \boldsymbol{\psi} \in \mathbf{V}.$$

Now, since $\mathbf{u} \in \mathbf{H}_0^1(\Omega)$ and $\mathbf{V} = \mathbf{H}(\text{div}, \Omega) \cap \mathbf{H}(\text{curl}, \Omega)$, integrating by parts yields

$$\int_{\Omega} (\nabla u_1 + \mathbf{curl} u_2) \cdot \boldsymbol{\psi} = \int_{\Omega} (-u_1 \text{div} \boldsymbol{\psi} + u_2 \text{curl} \boldsymbol{\psi}) \quad \forall \boldsymbol{\psi} \in \mathbf{V}.$$

Then, from the last two equations,

$$\int_{\Omega} (-u_1 \text{div} \boldsymbol{\psi} + u_2 \text{curl} \boldsymbol{\psi}) = \int_{\Omega} \frac{1}{V_P^2} \varphi_P \psi_P + \int_{\Omega} \frac{1}{V_S^2} \varphi_S \psi_S \quad \forall \boldsymbol{\psi} \in \mathbf{V}$$

and, hence, using (2.12) we derive that

$$\frac{1}{\omega^2} \left(\int_{\Omega} \text{div} \boldsymbol{\varphi} \text{div} \boldsymbol{\psi} + \int_{\Omega} \text{curl} \boldsymbol{\varphi} \text{curl} \boldsymbol{\psi} \right) = \int_{\Omega} \frac{1}{V_P^2} \varphi_P \psi_P + \int_{\Omega} \frac{1}{V_S^2} \varphi_S \psi_S.$$

Therefore, $(\omega, \boldsymbol{\varphi})$ is a solution to Problem 1. \square

The bilinear form $a(\cdot, \cdot)$ in Problem 1 is not elliptic. Indeed, this problem has an infinite-dimensional eigenspace \mathbf{K} associated to $\omega = 0$, which consists of all the div-free and curl-free vector fields:

$$\mathbf{K} := \{ \boldsymbol{\psi} \in \mathbf{V} : \text{div} \boldsymbol{\psi} = \text{curl} \boldsymbol{\psi} = 0 \text{ in } \Omega \}.$$

Let us emphasize that these eigenfunctions do not correspond to any physical vibration. They are just solutions to Problem 1 that appear in this formulation, but are not related to solutions of Problem 2 and, thus, they are not related to the actual vibration modes of the structure.

In turn, the solutions to Problem 1 with $\omega > 0$ can be seen as solutions in harmonic regime of the time-domain problem studied in [8] (see also [2, Section 2]), where a stable, energy preserving numerical scheme based on Lagrangian finite elements on quadrilateral grids is presented. In the same spirit, Problem 1 has been numerically solved with this kind of elements in [7, Section 3.5.2]. However, in the present case, spurious eigenvalues appear interspersed among the genuine approximations of the actual eigenvalues of the elasticity problem.

In Figure 1, we present numerical evidence of this behavior when lowest-order Lagrangian finite elements on triangular grids are used to solve Problem 1 on the unit square with physical parameters as in the numerical tests reported in Section 4. We show in this figure the vibration frequencies computed in the range $[0, 7.5]$, which contains approximations to the five smallest vibration frequencies of Problem 2, on four meshes with

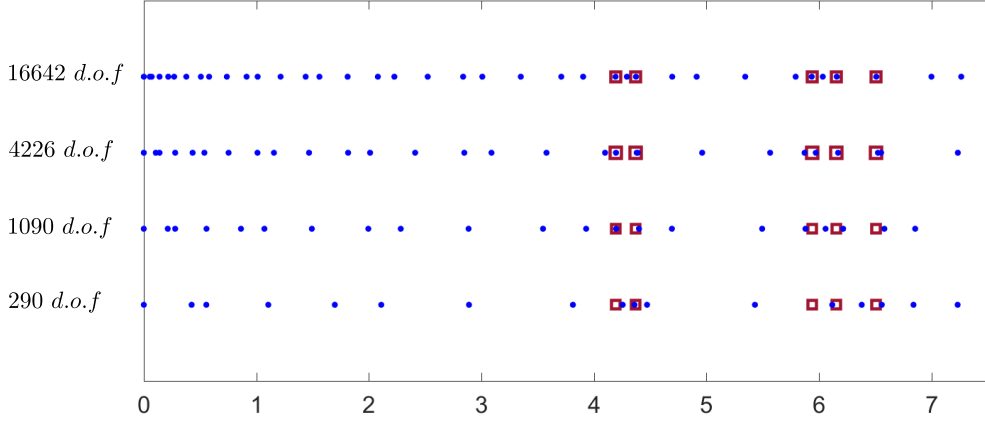


Figure 1: Vibration frequencies computed by solving Problem 2 (red squares) and Problem 1 (blue dots) with piecewise linear finite elements on four successively refined uniform meshes

different numbers of degrees of freedom (d.o.f.). We also include ‘exact’ vibration frequencies (see Section 4 for details). It can be clearly seen from this figure that discretizing this weak formulation with Lagrangian finite elements leads to spurious modes.

Let us remark that such spurious eigenvalues were expected to arise, since Problem 1 was numerically solved with a finite element discretization that yields approximations of the eigenfunctions in \mathbf{K} with non-vanishing discrete vibration frequencies $\omega_h > 0$. In such a case, when refining the mesh, these non-vanishing vibration frequencies get closer to zero, but new ones appear interspersed among the physically relevant ones. There are different techniques to try to circumvent this problem, for instance, to define a suitable numerical approximation that takes care of the eigenspace associated to $\omega = 0$ (see, [5, 6, 11, 12]) or to rewrite the problem in terms of an equivalent formulation in which 0 is not an eigenvalue (see, for instance, [13]). In this paper we will follow this last approach.

In the following section we will introduce two alternative variational formulations of Problem 1, which will be used for the theoretical analysis as well as for its finite element discretization. In these formulations, the eigenfunctions will be sought in a proper subspace of \mathbf{V} orthogonal to \mathbf{K} in a particular inner product. With this end, we will proceed as in [2] and establish a convenient decomposition of \mathbf{V} . We emphasize that the decomposition we are looking for is closely related with an elasticity problem with Dirichlet boundary conditions. In turn, the analysis proposed in [2] (see also [3]) relies on an elasticity problem with Neumann boundary conditions. Although our setting does not fit in [2], we will adapt its arguments to obtain the decomposition of \mathbf{V} .

3. Spurious modes free formulations

As claimed above, $\omega^2 = 0$ is an eigenvalue of Problem 1 with infinite-dimensional associated eigenspace

$$\mathbf{K} := \{\boldsymbol{\psi} \in \mathbf{V} : \operatorname{div} \boldsymbol{\psi} = \operatorname{curl} \boldsymbol{\psi} = 0 \quad \text{in } \Omega\}.$$

The remaining eigenfunctions, namely those corresponding to non-vanishing eigenvalues, are orthogonal to \mathbf{K} in the inner product $m(\cdot, \cdot)$. To prove this, let us define

$$\mathbf{G} := \mathbf{K}^{\perp m} := \{\boldsymbol{\varphi} \in \mathbf{V} : m(\boldsymbol{\varphi}, \boldsymbol{\psi}) = 0 \quad \forall \boldsymbol{\psi} \in \mathbf{K}\}.$$

Then, the following holds true:

Lemma 3.1. $\mathbf{V} = \mathbf{G} \oplus \mathbf{K}$, with \mathbf{G} and \mathbf{K} being orthogonal in the inner product $m(\cdot, \cdot)$.

PROOF. Given $\boldsymbol{\varphi} \in \mathbf{V}$, consider the following problem:

$$\text{Find } \boldsymbol{\varphi}_{\mathbf{K}} \in \mathbf{K} : \quad m(\boldsymbol{\varphi}_{\mathbf{K}}, \boldsymbol{\psi}) = m(\boldsymbol{\varphi}, \boldsymbol{\psi}) \quad \forall \boldsymbol{\psi} \in \mathbf{K}.$$

Since $m(\cdot, \cdot)^{1/2}$ is equivalent to the $L^2(\Omega)^2$ -norm, which in turn is equivalent to the \mathbf{V} -norm in \mathbf{K} , we have that $m(\cdot, \cdot)$ is elliptic in \mathbf{K} . Then, from Lax–Milgram lemma, the problem above has a unique solution $\boldsymbol{\varphi}_{\mathbf{K}} \in \mathbf{K}$. Let $\boldsymbol{\varphi}_{\mathbf{G}} := \boldsymbol{\varphi} - \boldsymbol{\varphi}_{\mathbf{K}}$. Then, $\boldsymbol{\varphi}_{\mathbf{G}} \in \mathbf{G}$ and $\boldsymbol{\varphi} = \boldsymbol{\varphi}_{\mathbf{G}} + \boldsymbol{\varphi}_{\mathbf{K}}$. Moreover, clearly $\boldsymbol{\varphi}_{\mathbf{G}}$ and $\boldsymbol{\varphi}_{\mathbf{K}}$ are m -orthogonal. \square

Now we are in a position to prove that the eigenfunctions corresponding to non-vanishing eigenvalues are orthogonal to \mathbf{K} .

Lemma 3.2. *If $(\omega, \boldsymbol{\varphi})$ is a solution to Problem 1 with $\omega > 0$, then $\boldsymbol{\varphi} \in \mathbf{G}$.*

PROOF. Let $(\omega, \boldsymbol{\varphi})$ be a solution to Problem 1 with $\omega > 0$. Then,

$$m(\boldsymbol{\varphi}, \boldsymbol{\psi}) = \frac{1}{\omega^2} a(\boldsymbol{\varphi}, \boldsymbol{\psi}) \quad \forall \boldsymbol{\psi} \in \mathbf{V}.$$

In particular, for all $\boldsymbol{\psi} \in \mathbf{K} \subset \mathbf{V}$, we have that $m(\boldsymbol{\varphi}, \boldsymbol{\psi}) = \frac{1}{\omega^2} a(\boldsymbol{\varphi}, \boldsymbol{\psi}) = 0$. Hence, $\boldsymbol{\varphi} \in \mathbf{G}$. \square

In what follows, we will show that the bilinear form $a(\cdot, \cdot)$, which is not elliptic in \mathbf{V} , is elliptic in \mathbf{G} . With this aim, we introduce a projector that will allow us to prove this fact, as well as some additional regularity of the functions in \mathbf{G} . Let

$$\begin{aligned} P : \mathbf{V} &\longrightarrow \mathbf{V}, \\ \varphi &\longmapsto \begin{pmatrix} V_P^2 \operatorname{div} \mathbf{u}_\varphi \\ -V_S^2 \operatorname{curl} \mathbf{u}_\varphi \end{pmatrix} \end{aligned}$$

with $\mathbf{u}_\varphi \in \mathbf{H}^1(\Omega)$ being the unique solution of the following standard linear elasticity Dirichlet problem with source term $-(\nabla \varphi_P + \mathbf{curl} \varphi_S) \in \mathbf{L}^2(\Omega)$:

$$-V_P^2 \nabla(\operatorname{div} \mathbf{u}_\varphi) + V_S^2 \mathbf{curl}(\operatorname{curl} \mathbf{u}_\varphi) = -(\nabla \varphi_P + \mathbf{curl} \varphi_S) \quad \text{in } \Omega, \quad (3.1a)$$

$$\mathbf{u}_\varphi = \mathbf{0} \quad \text{on } \partial\Omega. \quad (3.1b)$$

From classical additional regularity results for linear elasticity problems (see [10]), we know that there exists $\beta_0 > 0$, which depends on the domain and the Lamé coefficients, such that $\mathbf{u}_\varphi \in \mathbf{H}^{1+\beta}(\Omega)$ for all $\beta \in [0, \beta_0)$. Moreover, the following estimate holds true with a constant C independent of φ (notice that (2.9) has been used for the last equality):

$$\|\mathbf{u}_\varphi\|_{\mathbf{H}^{1+\beta}(\Omega)} \leq C \|\nabla \varphi_P + \mathbf{curl} \varphi_S\|_{\mathbf{L}^2(\Omega)} = C |\varphi|_{\mathbf{V}}. \quad (3.2)$$

From now on, we fix $\beta_0 > 0$ as the maximum number such that this estimate holds true for all $\beta \in [0, \beta_0)$.

It is easy to check that P is idempotent and hence a projector in \mathbf{V} , so that

$$\mathbf{V} = \operatorname{Im}(P) \oplus \operatorname{Ker}(P).$$

Moreover, we will show that its kernel is \mathbf{K} and its image is \mathbf{G} . Regarding the first one, having in mind (2.9), we have that

$$\forall \varphi \in \mathbf{V}, \quad P\varphi = \mathbf{0} \iff \nabla \varphi_P + \mathbf{curl} \varphi_S = \mathbf{0} \iff \begin{pmatrix} \operatorname{div} \varphi \\ \operatorname{curl} \varphi \end{pmatrix} = \mathbf{0} \iff \varphi \in \mathbf{K}.$$

Hence, $\operatorname{Ker}(P) = \mathbf{K}$. Therefore, in order to prove that the image of P is $\mathbf{G} := \mathbf{K}^{\perp m}$, it is enough to check that $\operatorname{Im}(P)$ and $\operatorname{Ker}(P)$ are orthogonal in the inner product $m(\cdot, \cdot)$.

Lemma 3.3. $\operatorname{Im}(P) \perp_m \operatorname{Ker}(P)$ and, consequently, $\operatorname{Im}(P) = \mathbf{G}$.

PROOF. Let $\varphi \in \mathbf{V}$. Let $\mathbf{u}_\varphi \in \mathbf{H}_0^1(\Omega)$ be the solution of (3.1). Then, for all $\psi \in \mathcal{D}(\overline{\Omega})^2$,

$$\begin{aligned} m(P\varphi, \psi) &= \int_{\Omega} \frac{1}{V_P^2} V_P^2 \operatorname{div} \mathbf{u}_\varphi \psi_P - \int_{\Omega} \frac{1}{V_S^2} V_S^2 \operatorname{curl} \mathbf{u}_\varphi \psi_S \\ &= - \int_{\Omega} \mathbf{u}_\varphi \cdot \nabla \psi_P - \int_{\Omega} \mathbf{u}_\varphi \cdot \mathbf{curl} \psi_S = - \int_{\Omega} \mathbf{u}_\varphi \cdot (\nabla \psi_P + \mathbf{curl} \psi_S). \end{aligned}$$

Since $\mathcal{D}(\overline{\Omega})^2$ is dense in \mathbf{V} , a standard density argument shows that the above equality holds for all $\psi \in \mathbf{V}$. In particular, for all $\psi \in \mathbf{K} \subset \mathbf{V}$, in whose case, by using (2.9), we derive that

$$m(P\varphi, \psi) = - \int_{\Omega} \mathbf{u}_\varphi \cdot \underbrace{(\nabla \psi_P + \mathbf{curl} \psi_S)}_{=0} = 0.$$

Hence, $\mathbf{V} = \operatorname{Im}(P) \overset{\perp m}{\oplus} \operatorname{Ker}(P) = \operatorname{Im}(P) \overset{\perp m}{\oplus} \mathbf{K}$. Then, since $\mathbf{V} = \mathbf{G} \overset{\perp m}{\oplus} \mathbf{K}$ too, it is easy to check that $\operatorname{Im}(P) = \mathbf{G}$. \square

Next step is to prove additional regularity for the functions in \mathbf{G} .

Lemma 3.4. *For all $\beta \in [0, \beta_0)$, $\mathbf{G} \subset \mathbf{H}^\beta(\Omega)$ and there exists $C > 0$ such that*

$$\|\varphi\|_{\mathbf{H}^\beta(\Omega)} \leq C |\varphi|_{\mathbf{V}} \quad \forall \varphi \in \mathbf{G}. \quad (3.3)$$

PROOF. Let $\varphi \in \mathbf{G} = \operatorname{Im}(P)$. Since P is a projector,

$$\varphi = P(\varphi) = \begin{pmatrix} V_P^2 \operatorname{div} \mathbf{u}_\varphi \\ -V_S^2 \operatorname{curl} \mathbf{u}_\varphi \end{pmatrix}$$

with \mathbf{u}_φ being the solution to (3.1). Then, according to (3.2),

$$\|\varphi\|_{\mathbf{H}^\beta(\Omega)} = V_P^2 \|\operatorname{div} \mathbf{u}_\varphi\|_{\mathbf{H}^\beta(\Omega)} + V_S^2 \|\operatorname{curl} \mathbf{u}_\varphi\|_{\mathbf{H}^\beta(\Omega)} \leq C \|\mathbf{u}_\varphi\|_{\mathbf{H}^{1+\beta}(\Omega)} \leq C |\varphi|_{\mathbf{V}}.$$

\square

Now we are in a position to prove the ellipticity of the bilinear form $a(\cdot, \cdot)$ in \mathbf{G} .

Corollary 3.5. *There exists $C > 0$ such that, for all $\varphi \in \mathbf{G}$,*

$$\|\varphi\|_{\mathbf{L}^2(\Omega)} \leq C |\varphi|_{\mathbf{V}}.$$

Consequently, $a(\cdot, \cdot)$ is elliptic in \mathbf{G} .

PROOF. The estimate is the particular case $\beta = 0$ of Lemma 3.4. The ellipticity follows immediately from the definition of $a(\cdot, \cdot)$ and this estimate. \square

We recall that we are looking for solutions φ in $\mathbf{G} = \mathbf{K}^{\perp m}$. With this in mind, we introduce a Lagrange multiplier which leads us to the following mixed spectral problem:

Problem 3. Find $(\omega, \varphi, \xi) \in \mathbb{R}^+ \times \mathbf{V} \times \mathbf{K}$ such that $(\varphi, \xi) \neq (\mathbf{0}, \mathbf{0})$ and

$$a(\varphi, \psi) + m(\xi, \psi) = \omega^2 m(\varphi, \psi) \quad \forall \psi \in \mathbf{V}, \quad (3.4a)$$

$$m(\varphi, \eta) = 0 \quad \forall \eta \in \mathbf{K}. \quad (3.4b)$$

Since $\mathbf{K} \subset \mathbf{V}$, from Corollary 3.5 it is straightforward to show that the bilinear forms $a(\cdot, \cdot)$ and $m(\cdot, \cdot)$ satisfy the Babuška-Brezzi conditions. Consequently, $\omega = 0$ is not an eigenvalue of this problem. Moreover, by taking $\psi = \xi \in \mathbf{K} \subset \mathbf{V}$, it follows that for any solution of Problem 3, $\xi = \mathbf{0}$.

From the previous assertions, it can be readily seen that if (ω, φ, ξ) is a solution of Problem 3, then $\omega \neq 0$ and (ω, φ) is a solution to Problem 1. Conversely, if (ω, φ) is a solution to Problem 1 with $\omega \neq 0$, then $(\omega, \varphi, \mathbf{0})$ is a solution to Problem 3. In the following section we will introduce a finite element discretization of Problem 3 and we will report numerical evidence that it does not introduce spurious modes. Before this, on the rest of this section, we will focus on the analysis of this formulation.

With this aim, we introduce the corresponding solution operator:

$$\begin{aligned} T : \mathbf{G} &\longrightarrow \mathbf{G}, \\ \mathbf{f} &\longmapsto T\mathbf{f} := \varphi \end{aligned}$$

with φ such that $(\varphi, \xi) \in \mathbf{V} \times \mathbf{K}$ satisfies

$$a(\varphi, \psi) + m(\xi, \psi) = m(\mathbf{f}, \psi) \quad \forall \psi \in \mathbf{V}, \quad (3.5a)$$

$$m(\varphi, \eta) = 0 \quad \forall \eta \in \mathbf{K}, \quad (3.5b)$$

Notice that (3.5b) implies that φ belongs to \mathbf{G} .

Since the bilinear forms $a(\cdot, \cdot)$ and $m(\cdot, \cdot)$ satisfy the Babuška-Brezzi conditions, (3.5) is a well posed mixed problem as stated in the following lemma:

Lemma 3.6. Let $\mathbf{f} \in \mathbf{G}$. Then, problem (3.5) has a unique solution $(\varphi, \xi) \in \mathbf{V} \times \mathbf{K}$. Moreover, $\xi = \mathbf{0}$ and there exists $C > 0$ independent of \mathbf{f} , such that

$$\|\varphi\|_{\mathbf{V}} \leq C \|\mathbf{f}\|_{\mathbf{L}^2(\Omega)}.$$

As a consequence of this lemma, it follows that the operator T is well-defined and bounded. Moreover, it is easy to check that 0 is not an eigenvalue of T . Furthermore, $T\boldsymbol{\varphi} = \kappa\boldsymbol{\varphi}$ with $\boldsymbol{\varphi} \neq \mathbf{0}$ if and only if there exists a solution $(\omega, \boldsymbol{\varphi}, \boldsymbol{\xi})$ of Problem 3 with $\omega = 1/\kappa \neq 0$. The following lemma shows additional regularity of the eigenfunctions of T , which will be subsequently used to obtain a spectral characterization of T .

Lemma 3.7. *Let $\mathbf{f} \in \mathbf{G}$ and $\boldsymbol{\varphi} = T\mathbf{f}$. Then, for all $\beta \in [0, \beta_0)$, there exists $C > 0$ such that*

$$\|\boldsymbol{\varphi}\|_{\mathbf{H}^\beta(\Omega)} + \|\operatorname{div} \boldsymbol{\varphi}\|_{\mathbf{H}^{1+\beta}(\Omega)} + \|\operatorname{curl} \boldsymbol{\varphi}\|_{\mathbf{H}^{1+\beta}(\Omega)} \leq C |\mathbf{f}|_{\mathbf{V}}. \quad (3.6)$$

Consequently, $T : \mathbf{G} \rightarrow \mathbf{G}$ is compact.

PROOF. Let $\mathbf{f} = (f_P, f_S)^\top \in \mathbf{G}$ and $\boldsymbol{\varphi} = T\mathbf{f}$. From (3.5b), it follows that $\boldsymbol{\varphi} \in \mathbf{G}$. Moreover, from Lemmas 3.4 and 3.6, it follows that for all $\beta \in [0, \beta_0)$, there exists $C > 0$ such that

$$\|\boldsymbol{\varphi}\|_{\mathbf{H}^\beta(\Omega)} \leq C |\boldsymbol{\varphi}|_{\mathbf{V}} \leq C \|\mathbf{f}\|_{\mathbf{L}^2(\Omega)} \leq C |\mathbf{f}|_{\mathbf{V}}, \quad (3.7)$$

the last inequality because of Corollary 3.5.

Next, we estimate the second and third terms on the left hand side of (3.6). Since $\mathbf{f} \in \mathbf{G}$, by taking $\boldsymbol{\psi} = \boldsymbol{\xi}$ in (3.5a), it follows from Lemma 3.1 that $\boldsymbol{\xi} = \mathbf{0}$. Moreover, from (3.5a) and (2.9), we have that $\boldsymbol{\varphi} = (\varphi_P, \varphi_S)^\top$ satisfies

$$\int_{\Omega} (\nabla\varphi_P + \operatorname{curl} \varphi_S) \cdot (\nabla\psi_P + \operatorname{curl} \psi_S) = \int_{\Omega} \frac{1}{V_P^2} f_P \psi_P + \int_{\Omega} \frac{1}{V_S^2} f_S \psi_S \quad \forall \boldsymbol{\psi} = (\psi_S, \psi_P)^\top \in \mathbf{V}.$$

Since $\mathcal{D}(\Omega)^2$ and $\mathcal{D}(\overline{\Omega})^2$ are subspaces of \mathbf{V} , by taking conveniently $\boldsymbol{\psi}$ in these subspaces and integrating by parts, we obtain

$$\begin{cases} -\operatorname{div}(\nabla\varphi_P + \operatorname{curl} \varphi_S) = \frac{f_P}{V_P^2} & \text{in } \Omega, \\ (\nabla\varphi_P + \operatorname{curl} \varphi_S) \cdot \mathbf{n} = 0 & \text{on } \partial\Omega \end{cases} \quad \text{and} \quad \begin{cases} \operatorname{curl}(\nabla\varphi_P + \operatorname{curl} \varphi_S) = \frac{f_S}{V_S^2} & \text{in } \Omega, \\ (\nabla\varphi_P + \operatorname{curl} \varphi_S) \cdot \mathbf{t} = 0 & \text{on } \partial\Omega. \end{cases} \quad (3.8)$$

Let $\tilde{\mathbf{u}} := \nabla\varphi_P + \operatorname{curl} \varphi_S = (\operatorname{div} \boldsymbol{\varphi}, -\operatorname{curl} \boldsymbol{\varphi})^\top$. Hence, from (2.9) again,

$$\begin{pmatrix} \operatorname{div} \tilde{\mathbf{u}} \\ -\operatorname{curl} \tilde{\mathbf{u}} \end{pmatrix} = \nabla \tilde{\mathbf{u}}_1 + \operatorname{curl} \tilde{\mathbf{u}}_2 = \nabla(\operatorname{div} \boldsymbol{\varphi}) - \operatorname{curl}(\operatorname{curl} \boldsymbol{\varphi}).$$

Thus, from (3.8), it follows that

$$-\nabla(\operatorname{div} \boldsymbol{\varphi}) + \operatorname{curl}(\operatorname{curl} \boldsymbol{\varphi}) = -\begin{pmatrix} \operatorname{div} \tilde{\mathbf{u}} \\ -\operatorname{curl} \tilde{\mathbf{u}} \end{pmatrix} = \begin{pmatrix} f_P/V_P^2 \\ f_S/V_S^2 \end{pmatrix} \quad (3.9)$$

and that $\tilde{\mathbf{u}} \in \mathbf{H}_0(\operatorname{div}, \Omega) \cap \mathbf{H}_0(\operatorname{curl}, \Omega) = \mathbf{H}_0^1(\Omega)$ (see [9, Lemma 2.5]). Consequently,

$$\operatorname{div} \boldsymbol{\varphi} = \operatorname{curl} \boldsymbol{\varphi} = 0 \quad \text{on } \partial\Omega. \quad (3.10)$$

Since $\mathbf{f} \in \mathbf{G} = \operatorname{Im}(P)$, we have that $\mathbf{f} = P\mathbf{f}$ and, hence, there exists $\mathbf{u}^{\mathbf{f}} \in \mathbf{H}_0^1(\Omega)$ such that

$$\mathbf{f} = \begin{pmatrix} V_P^2 \operatorname{div} \mathbf{u}^{\mathbf{f}} \\ -V_S^2 \operatorname{curl} \mathbf{u}^{\mathbf{f}} \end{pmatrix}. \quad (3.11)$$

In fact, $\mathbf{u}^{\mathbf{f}}$ is the solution of (3.1) with \mathbf{f} instead of $\boldsymbol{\varphi}$. Hence, from (3.2), $\mathbf{u}^{\mathbf{f}} \in \mathbf{H}^{1+\beta}(\Omega)$ and

$$\|\mathbf{u}^{\mathbf{f}}\|_{\mathbf{H}^{1+\beta}(\Omega)} \leq C \|\mathbf{f}\|_{\mathbf{V}}. \quad (3.12)$$

Now, (3.9), (3.10), (3.11), (2.9) and the fact that $\mathbf{u}^{\mathbf{f}} \in \mathbf{H}_0^1(\Omega)$ yield

$$\begin{aligned} -\nabla(\operatorname{div} \boldsymbol{\varphi}) + \operatorname{curl}(\operatorname{curl} \boldsymbol{\varphi}) &= \begin{pmatrix} \operatorname{div} \mathbf{u}^{\mathbf{f}} \\ -\operatorname{curl} \mathbf{u}^{\mathbf{f}} \end{pmatrix} = \nabla u_1^{\mathbf{f}} + \operatorname{curl} u_2^{\mathbf{f}} \quad \text{in } \Omega, \\ \operatorname{div} \boldsymbol{\varphi} = \operatorname{curl} \boldsymbol{\varphi} &= 0 \quad \text{and} \quad u_1^{\mathbf{f}} = u_2^{\mathbf{f}} = 0 \quad \text{on } \partial\Omega. \end{aligned}$$

Then, taking div and curl in the equations above, it is easy to check that $\operatorname{div} \boldsymbol{\varphi} = -u_1^{\mathbf{f}} \in \mathbf{H}_0^1(\Omega) \cap \mathbf{H}^{1+\beta}(\Omega)$ and $\operatorname{curl} \boldsymbol{\varphi} = u_2^{\mathbf{f}} \in \mathbf{H}_0^1(\Omega) \cap \mathbf{H}^{1+\beta}(\Omega)$. Thus, (3.6) is a consequence of (3.12) and (3.7).

Finally, from this additional regularity result and the compactness of the embedding $\mathbf{H}^\beta(\Omega) \hookrightarrow \mathbf{L}^2(\Omega)$, we conclude that the operator $T : \mathbf{G} \rightarrow \mathbf{G}$ is compact. \square

As a consequence of this result, it follows that the spectrum of T has 0 as its only accumulation point and that any nonzero point of the spectrum of T is an eigenvalue of finite multiplicity.

Moreover, it is easy to check that the solution operator T is self-adjoint with respect to the inner product $a(\cdot, \cdot)$. Since its spectrum is related with the solutions of Problem 3, we derive that this problem has a countable number of solutions $(\omega_n, \boldsymbol{\varphi}_n, \mathbf{0})$, $n \in \mathbb{N}$, with $\omega_n \rightarrow \infty$ and $\{\boldsymbol{\varphi}_n\}_{n \in \mathbb{N}}$ being a Hilbertian basis of \mathbf{G} .

We end this section, with a couple of useful characterizations of the space \mathbf{K} (cf. [3]). The first one relates \mathbf{K} with gradients of harmonic functions.

Remark 3.8. *It is easy to check that $\mathbf{K} = \nabla\mathcal{H}$, where $\mathcal{H} := \{p \in \mathbf{H}^1(\Omega) : \Delta p = 0 \text{ in } \Omega\}$ is the set of harmonic functions in Ω .*

The second one will be used in the following section to propose a discretization of \mathbf{K} .

Remark 3.9. *Let us consider the following subspace of $H^{-1/2}(\partial\Omega)$:*

$$M := \left\{ \nu \in H^{-1/2}(\partial\Omega) : \int_{\partial\Omega} \nu d\gamma = 0 \right\},$$

where, as usual, the integral over $\partial\Omega$ must be understood as the duality pairing $\langle \nu, 1 \rangle$ in $H^{-1/2}(\partial\Omega) \times H^{1/2}(\partial\Omega)$. We introduce the so-called **harmonic lifting operator**

$$\begin{aligned} \mathcal{E} : M &\longrightarrow \nabla\mathcal{H}, \\ \nu &\longmapsto \nabla p^\nu, \end{aligned} \tag{3.13}$$

where p^ν is the unique solution in $H^1(\Omega)/\mathbb{R}$ of the compatible Neumann problem

$$\begin{aligned} -\Delta p^\nu &= 0 \quad \text{in } \Omega, \\ \nabla p^\nu \cdot \mathbf{n} &= \nu \quad \text{on } \partial\Omega. \end{aligned}$$

The operator \mathcal{E} is an isomorphism from M onto $\nabla\mathcal{H} = \mathbf{K}$ endowed with the $\mathbf{L}^2(\Omega)$ -norm.

4. Finite element discretization

In this section, first we introduce a Galerkin approximation of Problem 3. With this purpose, we follow the approach from [3], which is based on discretizing the problem with standard Lagrange finite elements.

We assume that Ω is a polygonal domain with (open) edges denoted γ_j , $1 \leq j \leq J$, so that

$$\partial\Omega = \bigcup_{j=1}^J \bar{\gamma}_j \quad \text{and} \quad \gamma_k \cap \gamma_l = \emptyset \quad \text{if } k \neq l. \tag{4.14}$$

We recall that the finite element spaces for the two potentials can be constructed on different meshes, which yields additional flexibility to adapt the discretization to the behavior of each type of mode. Thus, we introduce three regular families of triangulations of Ω , $\{\mathcal{T}_{h_P}^P\}$, $\{\mathcal{T}_{h_S}^S\}$ and $\{\mathcal{T}_h\}$ with h_P , h_S and h being the respective mesh-sizes, which will be used for the discretization of the two potentials and the Lagrange multiplier, respectively. Of course the meshes do not need to be different; in practice, usually $\mathcal{T}_{h_P}^P$ is taken coarser than $\mathcal{T}_{h_S}^S$ and $\mathcal{T}_h = \mathcal{T}_{h_P}^P$.

Let us also recall that according to Proposition 2.2, classical discrete subspaces of $\mathbf{H}^1(\Omega)$ ensure an adequate approximation of \mathbf{V} . Thus, we choose the following standard

lowest-order Lagrange finite element spaces, which will be used for the discretization of the potentials φ_P, φ_S and the Lagrange multiplier $\boldsymbol{\xi}$, respectively:

$$\begin{aligned}\mathcal{L}_{h_P}^P &:= \{\varphi_h \in \mathcal{C}(\Omega) : \varphi_h|_K \in \mathbb{P}_1(K) \quad \forall K \in \mathcal{T}_{h_P}^P\}, \\ \mathcal{L}_{h_S}^S &:= \{\varphi_h \in \mathcal{C}(\Omega) : \varphi_h|_K \in \mathbb{P}_1(K) \quad \forall K \in \mathcal{T}_{h_S}^S\}, \\ \mathcal{L}_h &:= \{\varphi_h \in \mathcal{C}(\Omega) : \varphi_h|_K \in \mathbb{P}_1(K) \quad \forall K \in \mathcal{T}_h\}.\end{aligned}$$

The corresponding discrete space to approximate \mathbf{V} will be $\mathbf{V}_h := \mathcal{L}_{h_P}^P \times \mathcal{L}_{h_S}^S$. On the other hand, it is clear that some particular care has to be taken to build the discrete space \mathbf{K}_h approximating $\mathbf{K} = \nabla\mathcal{H}$. With this purpose, we take into account Remark 3.9 and build \mathbf{K}_h from a convenient discrete subspace M_h of M . The choice of M_h , which is a bit technical, is described below.

Given a subspace M_h of M , we consider the following discrete operator \mathcal{E}_h , which is a discrete version of the harmonic lifting operator \mathcal{E} defined in (3.13):

$$\begin{aligned}\mathcal{E}_h : M_h &\longrightarrow \mathbf{L}^2(\Omega), \\ \nu_h &\longmapsto \nabla p_h^{\nu_h},\end{aligned}$$

where $p_h^{\nu_h} \in \mathcal{L}_h$ is a solution of the following compatible Neumann problem:

$$\int_{\Omega} \nabla p_h^{\nu_h} \cdot \nabla q_h = \int_{\partial\Omega} \nu_h q_h d\gamma \quad \forall q_h \in \mathcal{L}_h.$$

Then, we will use $\mathbf{K}_h := \mathcal{E}_h(M_h)$ as the finite element discretization of \mathbf{K} .

Notice that \mathbf{K}_h is contained in $\mathbf{L}^2(\Omega)$ but not in \mathbf{V} , so that using \mathbf{K}_h to discretize \mathbf{K} leads to a non-conforming finite element approximation. Note as well that for \mathcal{E}_h to be an isomorphism from M_h onto \mathbf{K}_h , it is necessary to choose M_h so that the following property holds true:

$$\nu_h \in M_h : \int_{\partial\Omega} \nu_h q_h d\gamma = 0 \quad \forall q_h \in \mathcal{L}_h \quad \implies \quad \nu_h = 0.$$

There only remains to detail the choice of M_h . For this purpose and according to the definition of M in Remark 3.9, we use a classical choice in the context of mortar finite elements (see for instance [14]), in which discontinuities are allowed on the corners of the domain Ω .

We introduce $M_h \subset M$ as the space of traces of functions in \mathcal{L}_h , modified at the vertices of Ω , where we allow discontinuities and, at the same time, we reduce by 1 the polynomial order of functions in M_h along the two adjacent edges of the mesh that share each vertex of Ω .

To do this, we introduce a mesh $\mathcal{T}_h(\partial\Omega)$ as the trace of \mathcal{T}_h :

$$\mathcal{T}_h(\partial\Omega) := \{\ell \text{ edge of } K \in \mathcal{T}_h : \ell \subset \partial\Omega\}$$

and we separate the edges of $\mathcal{T}_h(\partial\Omega)$ into two disjoint groups:

$$\mathcal{T}_h(\partial\Omega) = \mathcal{T}_h^i(\partial\Omega) \cup \mathcal{T}_h^b(\partial\Omega).$$

The edges in $\mathcal{T}_h^b(\partial\Omega)$ are those that share a vertex with Ω , whereas the edges in $\mathcal{T}_h^i(\partial\Omega)$ are the remaining ones. Thus, we define the finite element space M_h as follows:

$$M_h := \left\{ \nu_h \in M : \nu_h \in \prod_{j=1}^J H^1(\gamma_j) \text{ such that } \nu_h|_\ell \in \mathbb{P}_1(\ell) \quad \forall \ell \in \mathcal{T}_h^i(\partial\Omega) \text{ and } \nu_h|_\ell \in \mathbb{P}_0(\ell) \quad \forall \ell \in \mathcal{T}_h^b(\partial\Omega) \right\}. \quad (4.15)$$

By using the above mentioned finite element spaces, we arrive at the following non-conforming approximation of Problem 3:

Problem 4. Find $(\omega_h, \boldsymbol{\varphi}_h, \boldsymbol{\xi}_h) \in \mathbb{R}^+ \times \mathbf{V}_h \times \mathbf{K}_h$ such that $(\boldsymbol{\varphi}_h, \boldsymbol{\xi}_h) \neq (\mathbf{0}, \mathbf{0})$ and

$$a(\boldsymbol{\varphi}_h, \boldsymbol{\psi}_h) + m(\boldsymbol{\xi}_h, \boldsymbol{\psi}_h) = \omega_h^2 m(\boldsymbol{\varphi}_h, \boldsymbol{\psi}_h) \quad \forall \boldsymbol{\psi}_h \in \mathbf{V}_h, \quad (4.16a)$$

$$m(\boldsymbol{\varphi}_h, \boldsymbol{\eta}_h) = 0 \quad \forall \boldsymbol{\eta}_h \in \mathbf{K}_h. \quad (4.16b)$$

Notice that contrary to the continuous case where $\mathcal{E}(M) = \mathbf{K} \subset \mathbf{V}$, in the discrete setting $\mathcal{E}_h(M_h) = \mathbf{K}_h \not\subset \mathbf{V}_h$. To the best of the authors' knowledge, a discrete inf-sup condition for $m(\cdot, \cdot)$ uniform in h has not been proved to hold in this setting.

Remark 4.1. *The simplest-minded choice of M_h would be to use continuous Lagrange finite elements on $\mathcal{T}_h(\partial\Omega)$. The reason why we have chosen the space M_h as defined in (4.15) is that using continuous Lagrange finite elements to build M_h fails in the context of elastodynamics with traction free boundary conditions (see [1, 2, 3]). However, we do not have any evidence that the same could happen in our vibration problem with Dirichlet boundary conditions. On the contrary, in such a case, some preliminary numerical results suggest that it would not fail. This simpler choice should be analyzed in a future work.*

5. Numerical experiments

Next, we report some numerical results that exhibit the absence of spurious modes and the approximation properties of the proposed scheme. With this end, we have implemented Problem 4 in a MATLAB code. We have applied this code to compute the smallest

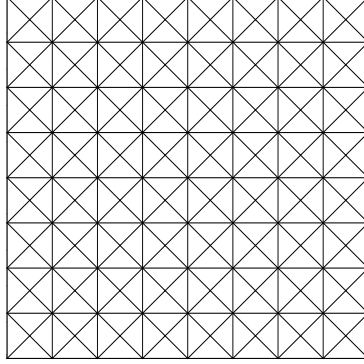


Figure 2: Uniform mesh on the unit square.

positive vibration frequencies in the unit square domain $\Omega = (0, 1)^2$ with density $\rho = 1$, Young modulus $E = 1$ and Poisson ratio $\nu = 0.35$. We recall that the Lamé coefficients are related to E and ν as follows:

$$\lambda := \frac{E\nu}{(1 + \nu)(1 - 2\nu)} \quad \text{and} \quad \mu := \frac{E}{2(1 + \nu)}.$$

Since no analytical solution is available, to validate the obtained results, we have used as a reference solution a finite element approximation of the classical displacement formulation (cf. Problem 2) computed on a very fine grid (525313 vertices), which we denote $(\omega_{\text{ref}}, \mathbf{u}_{\text{ref}})$.

For the first test, we have considered the same triangulations for all variables, namely, $\mathcal{T}_{hP}^P = \mathcal{T}_{hS}^S = \mathcal{T}_h$. In particular, we have used uniform meshes with different levels of refinement starting from that shown in Figure 2; we identify each mesh by the corresponding number N_h of vertices.

We have computed the smallest vibration frequencies on several meshes. Then, for each vibration frequency, we have extrapolated its computed values by means of a least-squares fitting to obtain what we denote ω_{ext} . Table 1 shows the results obtained for the seven smallest vibration frequencies $\{\omega_{i,h}\}_{i=1}^7$, as well as the corresponding extrapolated and reference values. It can be seen from this table that the proposed scheme approximates correctly the vibration frequencies of the elasticity problem and that no spurious value appears.

To appreciate the error of the eigenfunctions, we have computed the corresponding displacements from the potentials $\varphi_{P,h}$ and $\varphi_{S,h}$ as follows:

$$\mathbf{u}_h := \nabla \varphi_{P,h} + \mathbf{curl} \varphi_{S,h}.$$

Table 1: Smallest vibration frequencies computed by solving Problem 4 on different meshes.

N_h	41	145	545	2113	8321	33025	ω_{ext}	ω_{ref}
$\omega_{h,1}$	4.1641	4.2475	4.2126	4.2013	4.1971	4.1953	4.1950	4.1931
$\omega_{h,2}$	4.3384	4.2495	4.2131	4.2014	4.1971	4.1953	4.1950	4.1931
$\omega_{h,3}$	4.8001	4.4772	4.4000	4.3794	4.3740	4.3726	4.3722	4.3721
$\omega_{h,4}$	5.5047	6.0946	5.9828	5.9504	5.9403	5.9367	5.9362	5.9331
$\omega_{h,5}$	5.9930	6.3865	6.2154	6.1705	6.1589	6.1559	6.1551	6.1547
$\omega_{h,6}$	6.1424	6.3902	6.2161	6.1707	6.1589	6.1559	6.1551	6.1547
$\omega_{h,7}$	6.9931	6.8026	6.5792	6.5243	6.5104	6.5069	6.5063	6.5058

Table 2 shows the relative errors in $\mathbf{L}^2(\Omega)$ -norm of the computed displacements:

$$\|\mathbf{u}_{\text{ref}} - \mathbf{u}_h\|_{\mathbf{L}^2(\Omega)} / \|\mathbf{u}_{\text{ref}}\|_{\mathbf{L}^2(\Omega)},$$

for the 4 smallest eigenvalues on several meshes. It can be observed from this table that the relative errors get closer to zero as the number of degrees of freedom increases.

Table 2: Relative errors $\|\mathbf{u}_{\text{ref}} - \mathbf{u}_h\|_{\mathbf{L}^2(\Omega)} / \|\mathbf{u}_{\text{ref}}\|_{\mathbf{L}^2(\Omega)}$ of the displacements corresponding to the four smallest eigenvalues computed on different meshes.

N_h	145	545	2113	8321
$\omega_{h,1}$	0.1689	0.1109	0.0816	0.0630
$\omega_{h,2}$	0.1929	0.1144	0.0809	0.0622
$\omega_{h,3}$	0.1906	0.0883	0.0443	0.0234
$\omega_{h,4}$	0.2189	0.1283	0.0876	0.0654

In order to plot the computed displacements, we must have in mind that Problem 4 provides a piecewise linear numerical approximation of the potentials φ_P and φ_S , which leads to the piecewise constant approximation \mathbf{u}_h of the displacements. Then, to better compare computed and reference displacements, we have used for the former a standard post-processing operator \mathbf{I}_h , which computes piecewise linear displacements with nodal values obtained by averaging the piecewise constant displacements over all the elements sharing each node. In consequence, in what follows, to validate the numerical displacements obtained with the potentials approach, we will compare \mathbf{u}_{ref} with

$$\mathbf{I}_h \mathbf{u}_h = \mathbf{I}_h(\nabla \varphi_{P,h}) + \mathbf{I}_h(\mathbf{curl} \varphi_{S,h}).$$

Figure 3 shows uniform meshes deformed by the action of the corresponding displacement fields for the four smallest vibration frequencies. This figure includes deformations

produced by the post-processed computed displacement $\mathbf{I}_h(\nabla\varphi_{P,h})$, $\mathbf{I}_h(\mathbf{curl}\varphi_{S,h})$ and $\mathbf{I}_h\mathbf{u}_h$, as well as by the displacements of the reference solution \mathbf{u}_{ref} .

Let us remark that the meshes deformed by $\mathbf{I}_h\mathbf{u}_h$ and by \mathbf{u}_{ref} are very close, except around the corners of Ω for some vibration frequencies (in Figure 3, for $\omega_{h,1}$, $\omega_{h,2}$ and $\omega_{h,4}$). To better visualize the behavior of the computed displacements around these corners, we plot in Figure 4 the norm of the reference displacements $|\mathbf{u}_{\text{ref}}|$ and that of the computed displacements $|\mathbf{I}_h\mathbf{u}_h|$, corresponding to the smallest vibration frequency $\omega_{h,1}$ in both cases.

It can be seen from this figure that the post-processed computed displacements present peaks at the corners of the domain Ω . A similar behavior can be seen for the eigenfunctions corresponding to $\omega_{h,2}$ and $\omega_{h,4}$, but not for that corresponding to $\omega_{h,3}$. This behavior is not related to the type of mesh (criss-cross). In fact, we have tested with different meshes, both structured and unstructured, and the behavior at the corners does not change.

Let us remark that as the meshes are finer, the peaks at the corners become steeper. This phenomenon prevents convergence in \mathbf{V} -norm but not in $L^2(\Omega)$ -norm (cf. Table 2). In order to avoid this phenomenon, in what follows we propose an alternative finite element approximation of Problem 3.

To describe this alternative, let us first recall that $a(\boldsymbol{\xi}, \boldsymbol{\psi}) = 0$ for all $(\boldsymbol{\xi}, \boldsymbol{\psi}) \in \mathbf{K} \times \mathbf{V}$. Thus, the mass term in Problem 3 (cf. (3.4a)) can be equivalently written as follows:

$$m(\boldsymbol{\xi}, \boldsymbol{\psi}) = m(\boldsymbol{\xi}, \boldsymbol{\psi}) + a(\boldsymbol{\xi}, \boldsymbol{\psi}).$$

With this in mind, we introduce the following new finite element approximation of Problem 3:

Problem 5. Find $(\tilde{\omega}_h, \tilde{\boldsymbol{\varphi}}_h, \tilde{\boldsymbol{\xi}}_h) \in \mathbb{R}^+ \times \mathbf{V}_h \times \tilde{\mathbf{K}}_h$ such that $(\tilde{\boldsymbol{\varphi}}_h, \tilde{\boldsymbol{\xi}}_h) \neq (\mathbf{0}, \mathbf{0})$ and

$$\begin{aligned} a(\tilde{\boldsymbol{\varphi}}_h, \boldsymbol{\psi}_h) + \hat{m}(\tilde{\boldsymbol{\xi}}_h, \boldsymbol{\psi}_h) &= \tilde{\omega}_h^2 m(\tilde{\boldsymbol{\varphi}}_h, \boldsymbol{\psi}_h) \quad \forall \boldsymbol{\psi}_h \in \mathbf{V}_h, \\ \hat{m}(\tilde{\boldsymbol{\varphi}}_h, \tilde{\boldsymbol{\eta}}_h) &= 0 \quad \forall \tilde{\boldsymbol{\eta}}_h \in \tilde{\mathbf{K}}_h. \end{aligned}$$

In this problem,

$$\hat{m}(\boldsymbol{\varphi}_h, \boldsymbol{\psi}_h) := m(\boldsymbol{\varphi}_h, \boldsymbol{\psi}_h) + a(\boldsymbol{\varphi}_h, \boldsymbol{\psi}_h),$$

whereas $\tilde{\mathbf{K}}_h := \tilde{\Pi}_h \mathcal{E}_h(M_h)$ with $\tilde{\Pi}_h$ being the elliptic projection from $\mathbf{L}^2(\Omega)$ onto \mathbf{V}_h defined for any $\boldsymbol{\varphi} \in \mathbf{L}^2(\Omega)$ by

$$\tilde{\Pi}_h \boldsymbol{\varphi} \in \mathbf{V}_h : \int_{\Omega} \tilde{\Pi}_h \boldsymbol{\varphi} \cdot \boldsymbol{\psi}_h + a(\tilde{\Pi}_h \boldsymbol{\varphi}, \boldsymbol{\psi}_h) = m(\boldsymbol{\varphi}, \boldsymbol{\psi}_h) \quad \forall \boldsymbol{\psi}_h \in \mathbf{V}_h.$$

An interesting feature of this formulation is that, unlike Problem 4, it is straightforward to prove an inf-sup condition for the bilinear form $\hat{m}(\cdot, \cdot)$. This is a consequence of the inclusion $\tilde{\Pi}_h \mathcal{E}_h(M_h) \subset \mathbf{V}_h$.

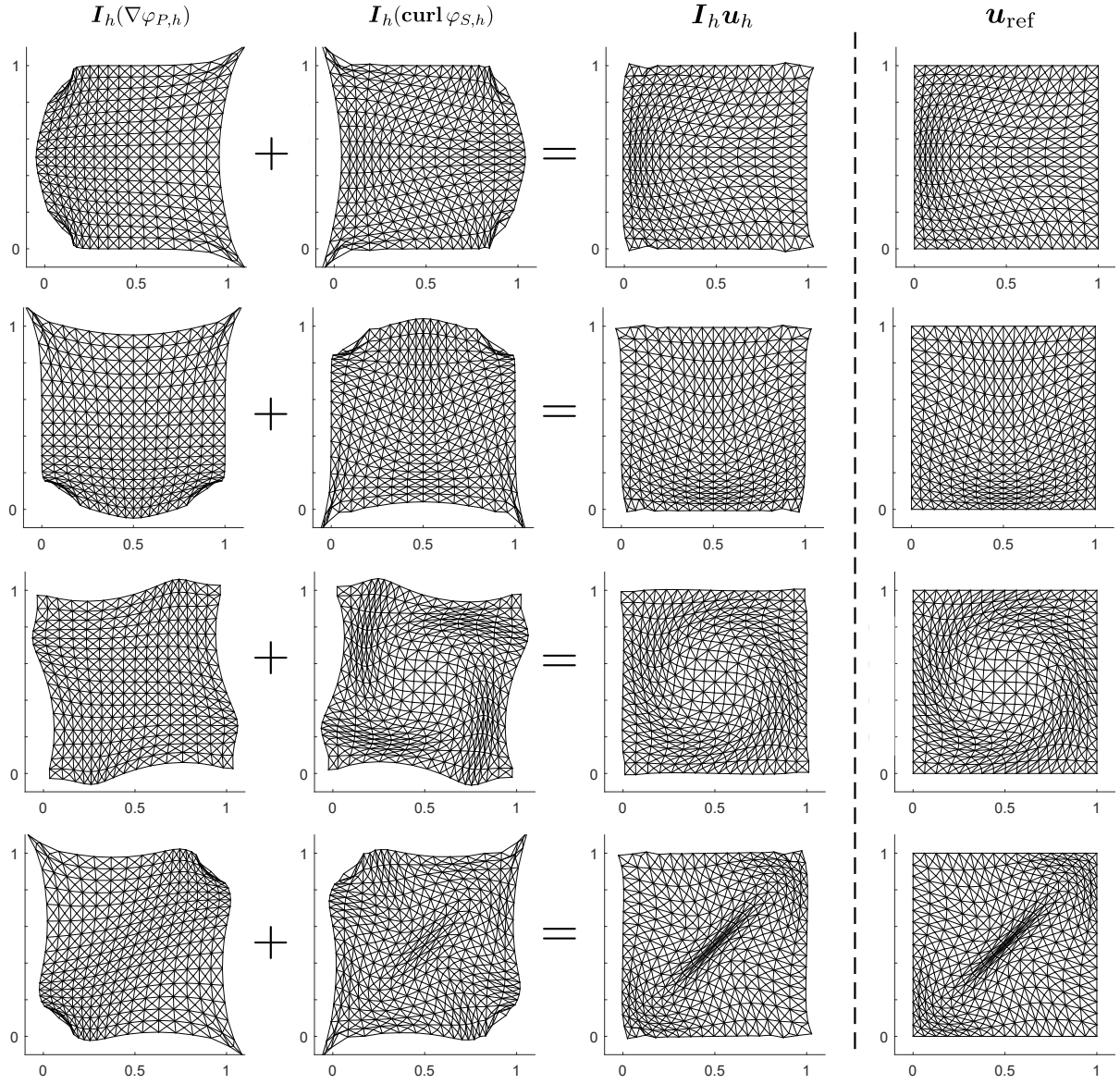


Figure 3: From left to right: Deformed meshes by the action of displacements $\mathbf{I}_h(\nabla\varphi_{P,h})$, $\mathbf{I}_h(\text{curl}\varphi_{S,h})$, $\mathbf{I}_h\mathbf{u}_h$ and \mathbf{u}_{ref} , corresponding to eigenvalues (from top to bottom) $\omega_{h,1}$, $\omega_{h,2}$, $\omega_{h,3}$ and $\omega_{h,4}$. Number of vertices $N_h = 545$.

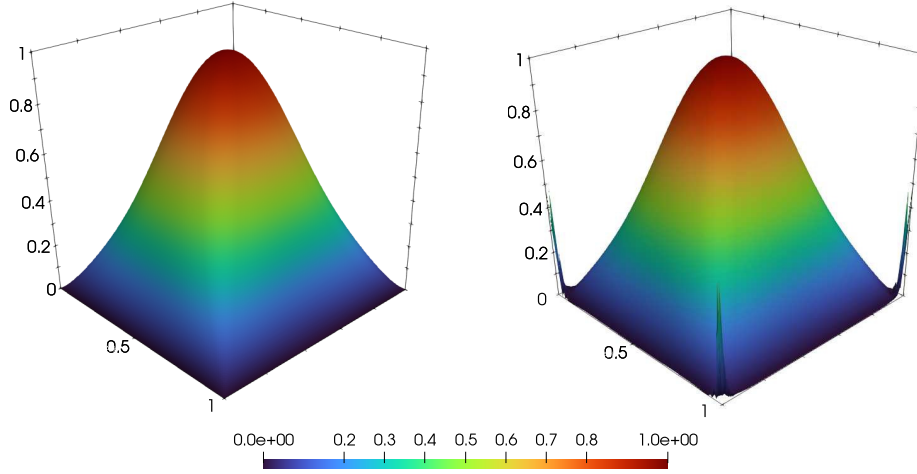


Figure 4: Norm of the reference displacement $|\mathbf{u}_{\text{ref}}|$ (left) and post-processed computed displacement $|\mathbf{I}_h \mathbf{u}_h|$ (right), corresponding to the vibration frequency $\omega_{h,1}$. Number of vertices $N_h = 20201$.

With this formulation both, vibration frequencies and eigenfunctions of the previous example, are approximated avoiding the peaks shown in Figure 4. This is reflected in Table 3 and Figures 5 and 6. In Table 3 the smallest seven vibration frequencies $\{\tilde{\omega}_{h,i}\}_{i=1}^7$ and the corresponding extrapolated values are shown and compared with the reference values for different meshes.

Table 3: Smallest positive vibration frequencies from Problem 5 computed on different meshes.

N_h	41	145	545	2113	8321	33025	$\tilde{\omega}_{\text{ext}}$	ω_{ref}
$\tilde{\omega}_{h,1}$	4.0955	4.1565	4.1776	4.1894	4.1924	4.1929	4.1948	4.1931
$\tilde{\omega}_{h,2}$	4.1523	4.1641	4.1785	4.1894	4.1924	4.1929	4.1956	4.1931
$\tilde{\omega}_{h,3}$	4.7400	4.4530	4.3906	4.3763	4.3731	4.3724	4.3722	4.3721
$\tilde{\omega}_{h,4}$	5.5111	5.9450	5.9329	5.9285	5.9316	5.9326	5.9310	5.9331
$\tilde{\omega}_{h,5}$	5.7878	6.3753	6.2067	6.1659	6.1567	6.1551	6.1542	6.1547
$\tilde{\omega}_{h,6}$	6.0711	6.3779	6.2069	6.1659	6.1567	6.1551	6.1542	6.1547
$\tilde{\omega}_{h,7}$	7.0052	6.5626	6.4705	6.4874	6.5046	6.5064	6.4920	6.5058

In Figures 5 and 6 we compare the reference displacements and the post-processed displacements computed by the potentials as follows:

$$\mathbf{I}_h \tilde{\mathbf{u}}_h = \mathbf{I}_h(\nabla \tilde{\varphi}_{P,h}) + \mathbf{I}_h(\mathbf{curl} \tilde{\varphi}_{S,h}).$$

Figure 5 shows the norm of the reference displacements (\mathbf{u}_{ref}) and the post-processed

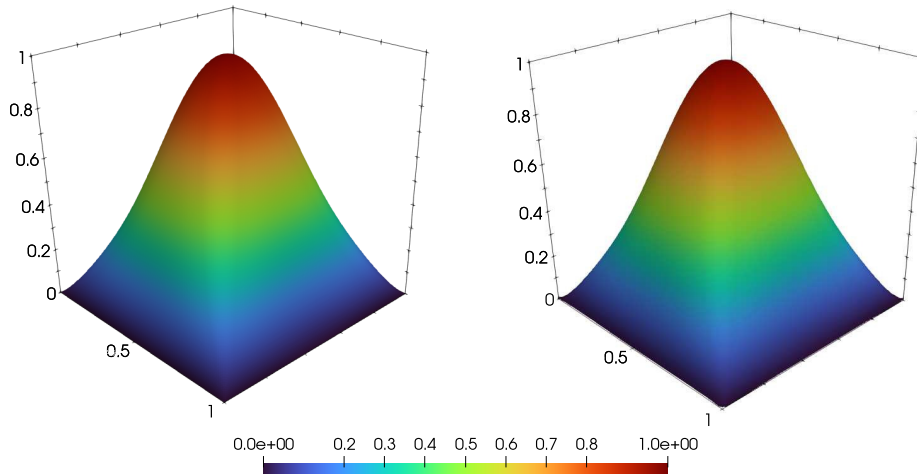


Figure 5: Norm of the reference displacements $|\mathbf{u}_{\text{ref}}|$ (left) and post-processed displacements $|\mathbf{I}_h \tilde{\mathbf{u}}_h|$ (right) corresponding to the vibration frequency $\omega_{h,1}$. Number of vertices $N_h = 20201$.

computed displacements $(\mathbf{I}_h \tilde{\mathbf{u}}_h)$ for the smallest vibration frequency $\omega_{h,1}$. We emphasize that the latter does not present any peak at the corners.

Figure 6 shows the meshes deformed under the action of the pressure and the shear motions computed with this method. A better approximation of the computed displacement field to the reference solution can be clearly observed.

To end this section, we check another property of the proposed numerical scheme. As explained in the introduction, the proposed method allows us to use different triangulations for each variable: $\mathcal{T}_{h_P}^P$ for the pressure potential φ_P , $\mathcal{T}_{h_S}^S$ for the shear potential φ_S and \mathcal{T}_h for the Lagrange multiplier. This is of interest, for example, when large displacements appear only in one of the potentials, since it leads to considering less degrees of freedom than with the classical displacement formulation.

As an example, we have solved Problem 5 with triangulations $\mathcal{T}_h = \mathcal{T}_{h_P}^P$ and $\mathcal{T}_{h_S}^S$ such that $2h_P = h_S$ and the same parameters as in the previous test. Figure 7 shows the meshes deformed under the action of the computed pressure motion $\mathbf{I}_h(\nabla \tilde{\varphi}_{P,h})$ and shear motion $\mathbf{I}_h(\mathbf{curl} \tilde{\varphi}_{S,h})$ for vibration frequencies $\tilde{\omega}_{h,8}$ and $\tilde{\omega}_{h,9}$. In the same figure, displacements \mathbf{u}_{ref} and $\tilde{\mathbf{u}}_h$ are also depicted. Let us remark that we have chosen these particular vibration frequencies because they are the smallest in which the displacements related with the pressure potential are small compared to those related with the shear potential (as can be seen from Figure 7). Thus, a coarser mesh can be used for φ_P . As in the previous examples, a good approximation of the reference displacement \mathbf{u}_{ref} can be clearly appreciated.

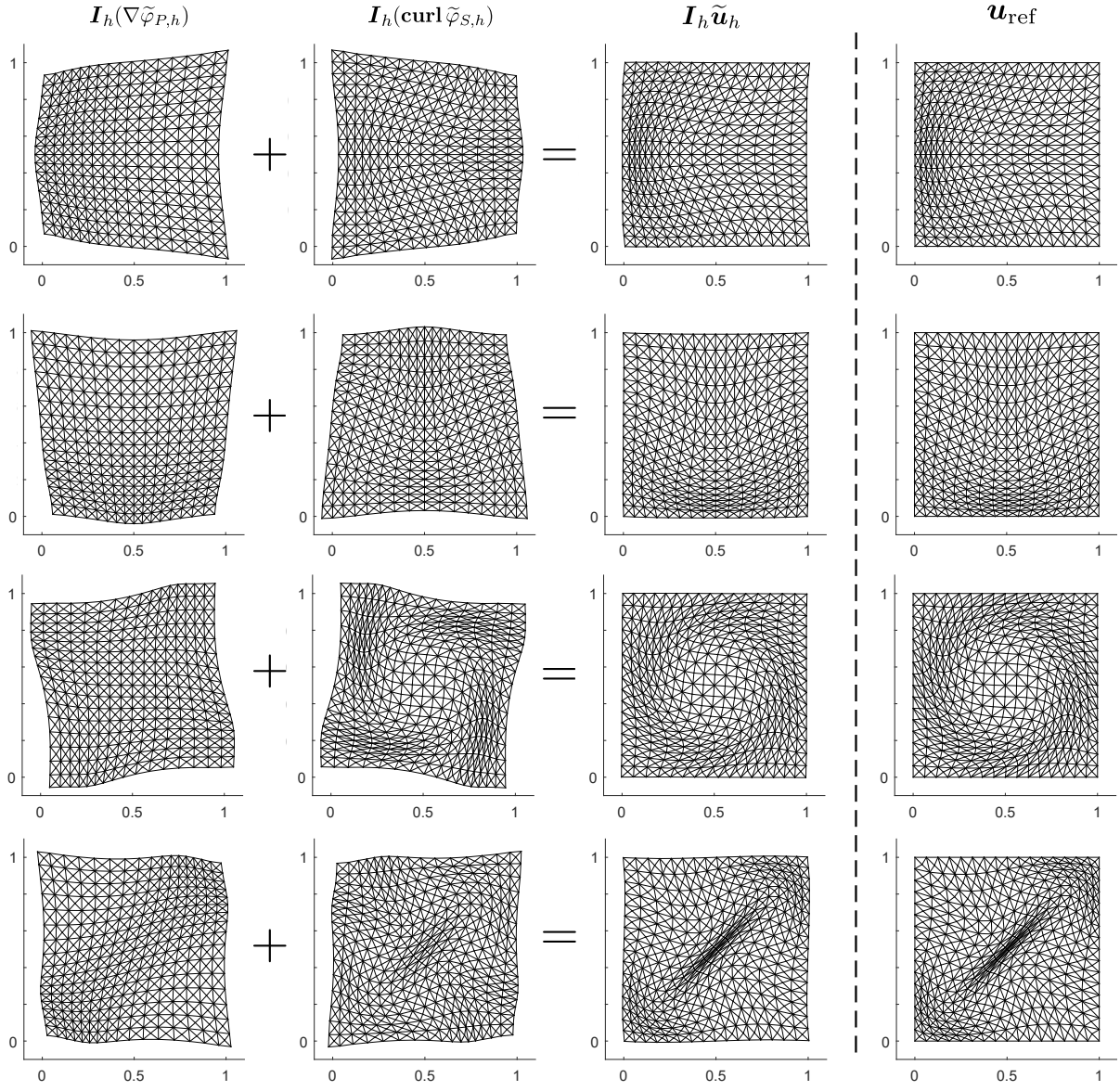


Figure 6: From left to right: Displacements $I_h(\nabla \tilde{\varphi}_{P,h})$, $I_h(\text{curl} \tilde{\varphi}_{S,h})$, $I_h \tilde{\mathbf{u}}_h$ and \mathbf{u}_{ref} corresponding to the vibration frequencies (from top to bottom) $\tilde{\omega}_{h,1}$, $\tilde{\omega}_{h,2}$, $\tilde{\omega}_{h,3}$ and $\tilde{\omega}_{h,4}$. Number of vertices $N_h = 545$.

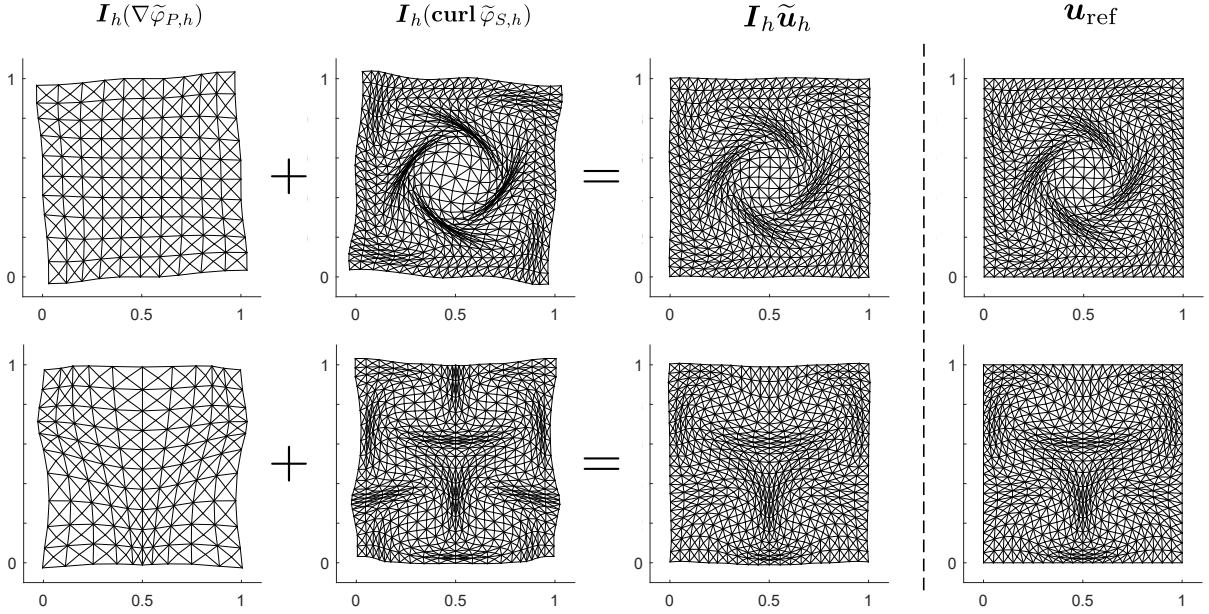


Figure 7: From left to right: Displacements $\mathbf{I}_h(\nabla \tilde{\varphi}_{P,h})$, $\mathbf{I}_h(\text{curl} \tilde{\varphi}_{S,h})$, $\mathbf{I}_h \tilde{\mathbf{u}}_h$ and \mathbf{u}_{ref} corresponding to the vibration frequencies $\tilde{\omega}_{h,8}$ (top) and $\tilde{\omega}_{h,9}$ (bottom). Number of vertices for $\mathcal{T}_{h_P}^P$ and $\mathcal{T}_{h_S}^S$ are 221 and 841, respectively.

Appendix

All the finite element approximations of Problem 3 introduced in the previous section require an appropriate discretization of the space \mathbf{K} . However, depending on the used computational tool, the finite element space for this discretization can be hard to implement, or even impossible in some platforms (for instance, FEniCS). In this appendix, we propose an alternative formulation whose discretization avoids the explicit use of \mathbf{K} , which leads to an easier implementation.

Problem 6. Find $(\omega, \boldsymbol{\varphi}, p, s) \in \mathbb{R} \times \mathbf{V} \times \mathbf{H}^1(\Omega)/\mathbb{R} \times \mathbf{H}_0^1(\Omega)$ such that $(\boldsymbol{\varphi}, p, s) \neq (\mathbf{0}, 0, 0)$ and

$$a(\boldsymbol{\varphi}, \boldsymbol{\psi}) + m(\nabla p, \boldsymbol{\psi}) = \omega^2 m(\boldsymbol{\varphi}, \boldsymbol{\psi}) \quad \forall \boldsymbol{\psi} \in \mathbf{V}, \quad (5.1a)$$

$$m(\boldsymbol{\varphi}, \nabla q) + (\nabla s, \nabla q)_{\mathbf{L}^2(\Omega)} = 0 \quad \forall q \in \mathbf{H}^1(\Omega)/\mathbb{R}, \quad (5.1b)$$

$$(\nabla p, \nabla r)_{\mathbf{L}^2(\Omega)} = 0 \quad \forall r \in \mathbf{H}_0^1(\Omega). \quad (5.1c)$$

Let us remark that we are using $(\cdot, \cdot)_{\mathbf{L}^2(\Omega)}$ to denote the standard inner product in $\mathbf{L}^2(\Omega)$. Notice that Problem 6 avoids the use of \mathbf{K} at the expense of introducing one

additional auxiliary variable. An advantage of this new formulation is that it can be easily solved by using general purpose finite element software packages like FEniCS. The following lemma shows that this mixed formulation is equivalent to Problem 3.

Lemma 5.1. *If $(\omega, \boldsymbol{\varphi}, \boldsymbol{\xi})$ is a solution to Problem 3, then there exist $p \in H^1(\Omega)/\mathbb{R}$ and $s \in H_0^1(\Omega)$ (depending on $\boldsymbol{\xi}$ and $\boldsymbol{\varphi}$, respectively) such that $(\omega, \boldsymbol{\varphi}, p, s)$ is a solution to Problem 6. Conversely, if $(\omega, \boldsymbol{\varphi}, p, s)$ is a solution to Problem 6, then $(\omega, \boldsymbol{\varphi}, \nabla p)$ is a solution to Problem 3.*

PROOF. Let $(\omega, \boldsymbol{\varphi}, p, s)$ be a solution to Problem 6. From (5.1c), we have that $\nabla p \in \mathbf{K}$. Therefore, $(\omega, \boldsymbol{\varphi}, \nabla p) \in \mathbb{R}^+ \times \mathbf{V} \times \mathbf{K}$ and it satisfies (3.4a). On the other hand, according to Remark 3.8, $\boldsymbol{\eta} \in \mathbf{K}$ if and only if there exists $q \in \mathcal{H} \subset H^1(\Omega)$ such that $\boldsymbol{\eta} = \nabla q$. Moreover, for each $q \in \mathcal{H}$, $(\nabla s, \nabla q)_{\mathbf{L}^2(\Omega)} = 0$. Then, $(\omega, \boldsymbol{\varphi}, \nabla p)$ also satisfies (3.4b) and, hence, it is a solution to Problem 3.

Conversely, let $(\omega, \boldsymbol{\varphi}, \boldsymbol{\xi})$ be a solution to Problem 3. Since $\boldsymbol{\xi} \in \mathbf{K}$, there exists $p \in \mathcal{H} \subset H^1(\Omega)$ such that $\boldsymbol{\xi} = \nabla p$. Then, $(\omega, \boldsymbol{\varphi}, p) \in \mathbb{R}^+ \times \mathbf{V} \times H^1(\Omega)/\mathbb{R}$ and it satisfies (5.1a) and (5.1c). It remains to show that there exists $s \in H_0^1(\Omega)$ such that (5.1b) holds true.

From (3.4b), we have that $\boldsymbol{\varphi} \in \mathbf{K}^{\perp m} = \mathbf{G}$. Then, $\boldsymbol{\varphi} = P\boldsymbol{\varphi} = \begin{pmatrix} V_P^2 \operatorname{div} \mathbf{u}^\varphi \\ -V_S^2 \operatorname{curl} \mathbf{u}^\varphi \end{pmatrix}$ with $\mathbf{u}^\varphi \in \mathbf{H}_0^1(\Omega)$ being the solution of (3.1). Hence,

$$\begin{pmatrix} \varphi_P/V_P^2 \\ \varphi_S/V_S^2 \end{pmatrix} = \begin{pmatrix} \operatorname{div} \mathbf{u}^\varphi \\ -\operatorname{curl} \mathbf{u}^\varphi \end{pmatrix} = \nabla u_1^\varphi + \mathbf{curl} u_2^\varphi \quad \text{in } \Omega.$$

Consequently,

$$m(\boldsymbol{\varphi}, \nabla q) = \int_{\Omega} (\nabla u_1^\varphi + \mathbf{curl} u_2^\varphi) \cdot \nabla q = \int_{\Omega} \nabla u_1^\varphi \cdot \nabla q \quad \forall q \in H^1(\Omega),$$

the last equality because $\mathbf{curl}(H_0^1(\Omega)) = H_0(\operatorname{div}^0, \Omega)$. Then, $m(\boldsymbol{\varphi}, \nabla q) = -(\nabla s, \nabla q)_{\mathbf{L}^2(\Omega)}$ with $s := -u_1^\varphi \in H_0^1(\Omega)$, so that (5.1b) holds true. Then, $(\omega, \boldsymbol{\varphi}, p, s)$ is a solution to Problem 6. \square

To introduce a Galerkin approximation of Problem 6, we consider the finite element spaces $\mathbf{V}_h \subset \mathbf{V}$, $\mathcal{L}_h \subset H^1(\Omega)$ defined in Section 4 and $\mathcal{L}_h^0 := \mathcal{L}_h \cap H_0^1(\Omega)$. Thus, we are lead to the following discretization of Problem 6:

Problem 7. Find $(\widehat{\omega}_h, \widehat{\varphi}_h, p_h, s_h) \in \mathbb{R} \times \mathbf{V}_h \times \mathcal{L}_h/\mathbb{R} \times \mathcal{L}_h^0$ such that $(\widehat{\varphi}_h, p_h, s_h) \neq (\mathbf{0}, 0, 0)$ and

$$a(\widehat{\varphi}_h, \boldsymbol{\psi}_h) + m(\nabla p_h, \boldsymbol{\psi}_h) = \widehat{\omega}_h^2 m(\widehat{\varphi}_h, \boldsymbol{\psi}_h) \quad \forall \boldsymbol{\psi}_h \in \mathbf{V}_h, \quad (5.2a)$$

$$m(\widehat{\varphi}_h, \nabla q_h) + (\nabla s_h, \nabla q_h) = 0 \quad \forall q_h \in \mathcal{L}_h/\mathbb{R}, \quad (5.2b)$$

$$(\nabla p_h, \nabla r_h) = 0 \quad \forall r_h \in \mathcal{L}_h^0. \quad (5.2c)$$

We conclude this section by noting that, although the numerical schemes (4.16a)–(4.16b) and (5.2a)–(5.2c) are not equivalent, we obtain similar results with both formulations. For example, in Table 4 we report the 4 smallest computed vibration frequencies $\{\widehat{\omega}_{h,i}\}_{i=1}^4$ and $\{\omega_{h,i}\}_{i=1}^4$ in the unit square, obtained by solving Problems 4 and 7, respectively. It can be seen from this table that the vibration frequencies of the elasticity problem are well approximated by solving Problem 7 and that this method is free of spurious modes.

The displacements computed from the eigenfunctions of Problem 7 also have the same drawbacks than those computed from Problem 4: they converge in $\mathbf{L}^2(\Omega)$ but have steep peaks at the corners of the domain Ω , which prevents convergence in \mathbf{V} . However, this can be also fixed by proceeding as in Section 4.

Table 4: Smallest positive vibration frequencies from Problems 4 and 7 computed on different meshes.

N_h	41	145	545	2113	8321	33025	ω_{ext}
$\omega_{h,1}$	4.1641	4.2475	4.2126	4.2013	4.1971	4.1953	4.1950
$\widehat{\omega}_{h,1}$	4.3443	4.2595	4.2230	4.2079	4.2011	4.1978	4.1960
$\omega_{h,2}$	4.3384	4.2495	4.2131	4.2014	4.1971	4.1953	4.1950
$\widehat{\omega}_{h,2}$	4.4450	4.2780	4.2248	4.2081	4.2013	4.1978	4.1976
$\omega_{h,3}$	4.8001	4.4772	4.4000	4.3794	4.3740	4.3726	4.3722
$\widehat{\omega}_{h,3}$	4.8007	4.4801	4.4005	4.3794	4.3740	4.3726	4.3721
$\omega_{h,4}$	5.5047	6.0946	5.9828	5.9504	5.9403	5.9367	5.9362
$\widehat{\omega}_{h,4}$	6.5274	6.1278	5.9993	5.9601	5.9462	5.9403	5.9397

6. Conclusions

We have proposed numerical schemes to solve a potentials formulation of the elasticity eigenvalue problem. We have shown that, spurious eigenvalues appear when lowest-order Lagrangian finite elements are used to discretize the problem. Although this type of element has been used in the elastodynamics setting, this behavior has not been documented.

In this work we have introduced two mixed formulations which allowed us to avoid this drawback. The discretizations are based on Lagrangian finite elements for the potentials and the auxiliary variables. We have reported several illustrative numerical examples that allowed us to assess the convergence properties of the method and to check that it is not polluted with spurious modes.

Acknowledgements

J. Albella was supported by FEDER / Ministerio de Ciencia, Innovación y Universidades and Agencia Estatal de Investigación through grants MTM2013-43745-R and MTM2017-86459-R and by Xunta de Galicia through grant ED431C 2017/60. R. Rodríguez was partially supported by Centro de Modelamiento Matemático (CMM), FB210005 BASAL funds for centers of excellence from ANID-Chile. P. Venegas was partially supported by FONDECYT-Chile project 1211030, Centro de Modelamiento Matemático (CMM), FB210005, BASAL funds for centers of excellence from ANID-Chile and by DIUBB through projects 2020126 IF/R and 2120173 GI/C

References

- [1] J. Albella. *Advanced numerical methods for wave propagation problems The Arlequin method and Potential formulation for elastodynamics*. PhD thesis, Universidade de Santiago de Compostela, 2019.
- [2] J. Albella, S. Imperiale, P. Joly, and J. Rodríguez. Solving 2D linear isotropic elastodynamics by means of scalar potentials: a new challenge for finite elements. *J. Sci. Comput.*, 77(3):1832–1873, 2018.
- [3] J. Albella, S. Imperiale, P. Joly, and J. Rodríguez. Numerical analysis of a method for solving 2D linear isotropic elastodynamics with traction free boundary condition using potentials and finite elements. *Math. Comp.*, 90(330):1589–1636, 2021.
- [4] C. Amrouche, C. Bernardi, M. Dauge, and V. Girault. Vector potentials in three-dimensional non-smooth domains. *Math. Methods Appl. Sci.*, 21(9):823–864, 1998.
- [5] A. Bermúdez, R. Durán, M. A. Muschietti, R. Rodríguez, and J. Solomin. Finite element vibration analysis of fluid-solid systems without spurious modes. *SIAM J. Numer. Anal.*, 32(4):1280–1295, 1995.
- [6] D. Boffi, R. G. Duran, and L. Gastaldi. A remark on spurious eigenvalues in a square. *Appl. Math. Lett.*, 12(3):107–114, 1999.

- [7] A. Burel. *Contributions à la simulation numérique en élastodynamique : découplage des ondes P et S, modèles asymptotiques pour la traversée de couches minces*. Theses, Université Paris Sud - Paris XI, 2014.
- [8] A. Burel, S. Imperiale, and P. Joly. Solving the homogeneous isotropic linear elastodynamics equations using potentials and finite elements. The case of the rigid boundary condition. *Numer. Anal. Appl.*, 5(2):136–143, 2012.
- [9] V. Girault and P.-A. Raviart. *Finite element methods for Navier-Stokes equations*, volume 5 of *Springer Series in Computational Mathematics*. Springer-Verlag, Berlin, 1986. Theory and algorithms.
- [10] P. Grisvard. *Elliptic Problems in Nonsmooth Domains*, volume 69 of *Classics in Applied Mathematics*. Society for Industrial and Applied Mathematics (SIAM), Philadelphia, PA, 2011.
- [11] H. Morand and R. Ohayon. *Fluid Structure Interaction*. J. Wiley and Sons, Chichester, 1995.
- [12] J. Querales, R. Rodríguez, and P. Venegas. Numerical approximation of the displacement formulation of the axisymmetric acoustic vibration problem. *SIAM J. Sci. Comput.*, 43(3):A1583–A1606, 2021.
- [13] J. Querales and P. Venegas. Mixed approximation of the axisymmetric acoustic eigenvalue problem. *Comput. Math. Appl.*, 108:1–11, 2022.
- [14] B. Wohlmuth. *Discretization methods and iterative solvers based on domain decomposition*, volume 17 of *Lecture Notes in Computational Science and Engineering*. Springer-Verlag, Heidelberg, 2001.

Centro de Investigación en Ingeniería Matemática (CI²MA)

PRE-PUBLICACIONES 2022

- 2022-17 FELIPE LEPE, DAVID MORA, GONZALO RIVERA, IVÁN VELÁSQUEZ: *A posteriori virtual element method for the acoustic vibration problem*
- 2022-18 FRANZ CHOULY: *A review on some discrete variational techniques for the approximation of essential boundary conditions*
- 2022-19 VERONICA ANAYA, RUBEN CARABALLO, SERGIO CAUCAO, LUIS F. GATICA, RICARDO RUIZ-BAIER, IVAN YOTOV: *A vorticity-based mixed formulation for the unsteady Brinkman-Forchheimer equations*
- 2022-20 OLGA BARRERA, STÉPHANE P. A. BORDAS, RAPHAËL BULLE, FRANZ CHOULY, JACK S. HALE: *An a posteriori error estimator for the spectral fractional power of the Laplacian*
- 2022-21 STÉPHANE P. A. BORDAS, RAPHAËL BULLE, FRANZ CHOULY, JACK S. HALE, ALEXEI LOZINSKI: *Hierarchical a posteriori error estimation of Bank–Weiser type in the Fenics project*
- 2022-22 FRANZ CHOULY, PATRICK HILD, VANESSA LLERAS, YVES RENARD: *Nitsche method for contact with Coulomb friction: existence results for the static and dynamic finite element formulations*
- 2022-23 FRANZ CHOULY, PATRICK HILD: *On a finite element approximation for the elastoplastic torsion problem*
- 2022-24 RAIMUND BÜRGER, STEFAN DIEHL, MARÍA CARMEN MARTÍ, YOLANDA VÁSQUEZ: *A difference scheme for a triangular system of conservation laws with discontinuous flux modeling three-phase flows*
- 2022-25 RAIMUND BÜRGER, HAROLD D. CONTRERAS, LUIS M. VILLADA: *A Hilliges-Weidlich-type scheme for a one-dimensional scalar conservation law with nonlocal flux*
- 2022-26 CLAUDIO I. CORREA, GABRIEL N. GATICA, RICARDO RUIZ-BAIER: *New mixed finite element methods for the coupled Stokes and Poisson-Nernst-Planck equations in Banach spaces*
- 2022-27 RODOLFO ARAYA, CRISTIAN CÁRCAMO, ABNER POZA: *A stabilized finite element method for the Stokes–Temperature coupled problem*
- 2022-28 JORGE ALBELLA, RODOLFO RODRÍGUEZ, PABLO VENEGAS: *Numerical approximation of a potentials formulation for the elasticity vibration problem*

Para obtener copias de las Pre-Publicaciones, escribir o llamar a: DIRECTOR, CENTRO DE INVESTIGACIÓN EN INGENIERÍA MATEMÁTICA, UNIVERSIDAD DE CONCEPCIÓN, CASILLA 160-C, CONCEPCIÓN, CHILE, TEL.: 41-2661324, o bien, visitar la página web del centro: <http://www.ci2ma.udec.cl>



**CENTRO DE INVESTIGACIÓN EN
INGENIERÍA MATEMÁTICA (CI²MA)
Universidad de Concepción**



Casilla 160-C, Concepción, Chile
Tel.: 56-41-2661324/2661554/2661316
<http://www.ci2ma.udec.cl>

